

CHAPTER II

LITERATURE REVIEW

1. THE MODEL DRUG

Figure 1 shows a molecule as spherical 3D of clopidogrel bisulfate ($C_{16}H_{16}ClNO_2S \cdot H_2SO_4$) or scientific name called methyl(+)-(S)- α -(2-chlorophenyl)-4,5,6,7-tetra-hydrothieno [3,2-c] pyridine-5-acetate hydrogen sulphate which is an antiplatelet drug used to inhibit platelet aggregation or blood clot in vascular diseases. The mechanism of action of this medicine is a selective and irreversible inhibitor at adenosine diphosphate (ADP) receptor on platelet's cell membrane induced platelet aggregation. This ADP receptor is called P2Y₁₂ which is initiate of the cross-linking of platelets by fibrin (7).

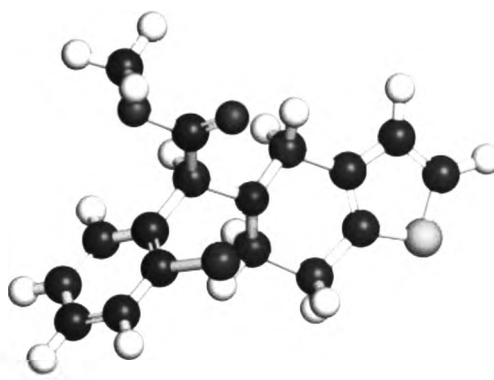


Figure 1 A molecule of clopidogrel bisulfate (Each atoms represents with typical color coding such as hydrogen (white), carbon (grey), nitrogen (blue), oxygen (red), sulfur (yellow) or chlorine (green) (8)

Clopidogrel bisulfate is a thienopyridine derivative having chemical structure relate to ticlopidine. Molecular structure of thienopyridine derivative contain an

asymmetric at carbon 8 (C8) position leading to the existence of two enantiomers (R-from and S-from) (7). Figure 2 indicates a chemical structure of S-enantiomer clopidogrel or scientific name called (S)-(+)-methyl (2-chlorophenyl)(6,7-dihydro-4H-thienol [3,2-c]pyridine-5-yl) acetate. This enantiomer (S-enantiomer) is a potent drug. On the other hand, R-enantiomer at C8 position does not exhibit antiplatelet aggregation activity. The carboxylic acid derivative of clopidogrel (clopidogrel acid, COOH) or scientific name called (S)-(+)-methyl (2-chlorophenyl)(6,7-dihydro-4H-thienol[3,2-c]pyridine-5-yl) acetic acid can be obtained from the hydrolysis reaction of the ester group at carbon 16 (C16) position. The hydrolysis reaction at this position is the main degradation product which does not exhibit pharmacological activity. In vitro study, the hydrolysis of ester group is catalyzed by higher temperature or higher humidity or both condition. Whereas in vivo study, the hydrolysis of ester group is caused by the action of enzyme carboxylesterase (9).

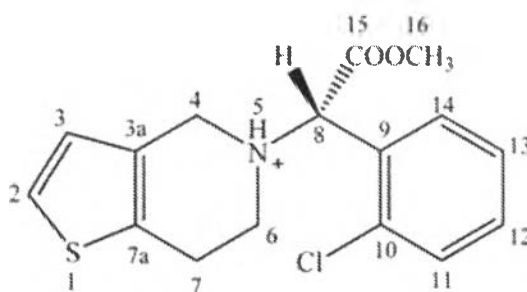


Figure 2 A chemical structure of clopidogrel (S-enantiomer) (9)

Clopidogrel bisulfate is an antiplatelet drug which is available in oral solid dosage form on the market (Plavix[®]). There are six different polymorphs for this drug that are known, but only two polymorphs such as Form I and Form II are commercially utilized. Both forms of known polymorph have almost similar



bioavailability (6). Bousquet report in US patent No. 6504030 B1 that clopidogrel bisulfate polymorph Form I is a monoclinic space group and has melting point at 184°C . On the contrary, clopidogrel bisulfate polymorph Form II is an orthorhombic space group and has melting point at 176°C . Polymorph Form II is characterized as bulk solid which is more compact and much less electrostatic the Form I. Moreover, polymorph Form II shows a lower solubility and greater thermodynamic stability than Form I (10). Figure 3a exhibits SEM micrographs of clopidogrel bisulfate polymorph Form I which shows irregular columnar aggregated particles shape of different sizes. On the contrary, Figure 3b exhibits SEM micrographs of clopidogrel bisulfate polymorph Form II which shows big round agglomerated form from sticky plates seen in powder (9).

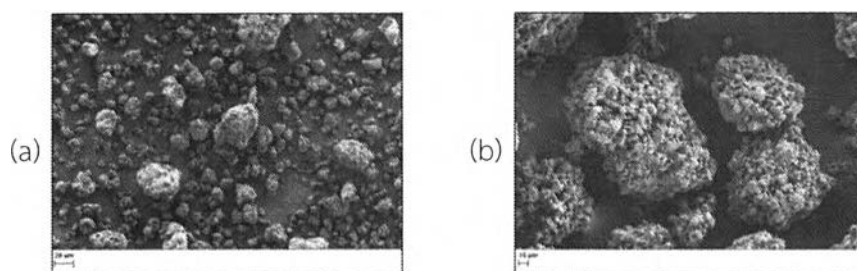


Figure 3 SEM micrographs of clopidogrel bisulfate Form I (a) Form II (b) (9)

Figure 4 exhibits the crystallographic structure of clopidogrel bisulfate polymorph Form II. It comprises a part of crystallographically independent clopidogrel cation and another part of bisulfate anion pair. A asymmetric unit of clopidogrel bisulfate polymorph Form II consists of clopidogrel cation and sulfate anion pair caused by transfer a proton bonded to the nitrogen. This molecular structure is stabilized by chains of sulfate ions along the C axis linked by hydrogen bonds (7).

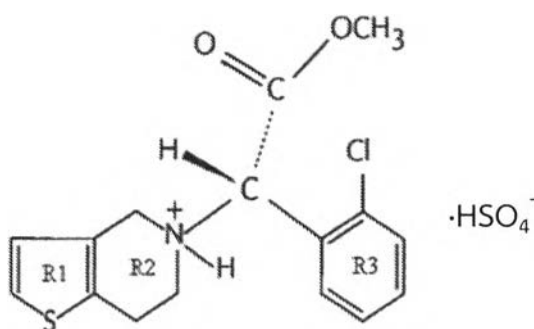


Figure 4 A chemical structure of clopidogrel bisulfate polymorph Form II (7)

More researchers reported that clopidogrel bisulfate had several polymorphs. Rajjada report that there are two solid polymorphs Forms (Form I and II) are commercial used by powder X-ray diffraction (PXRD) patterns. These results are shown in Figure 5. Clopidogrel polymorph Form I exhibits PXRD characteristic peaks at 9.2° and 12.2° 2θ , while polymorph Form II shows PXRD characteristic peaks at 8.91° and 12.42° 2θ (11). Uvarov et al. confirm this experimental data that the two solid polymorphs Forms used commercially by PXRD patterns. These results are shown in Figure 6. Figure 6a exhibits the PXRD pattern of clopidogrel bisulfate polymorph Form I composed of d-spacing value with 8.13 \AA , 5.98 \AA and 4.32 \AA . Figure 6b shows the PXRD pattern of clopidogrel bisulfate polymorph Form II composed of d-spacing values with 7.24 \AA and 6.88 \AA . Figure 6c indicates the mixture of two polymorphs Forms. This experiment report that only a few intensive peaks do not overlap and can be used for the quantification by the direct method (12).



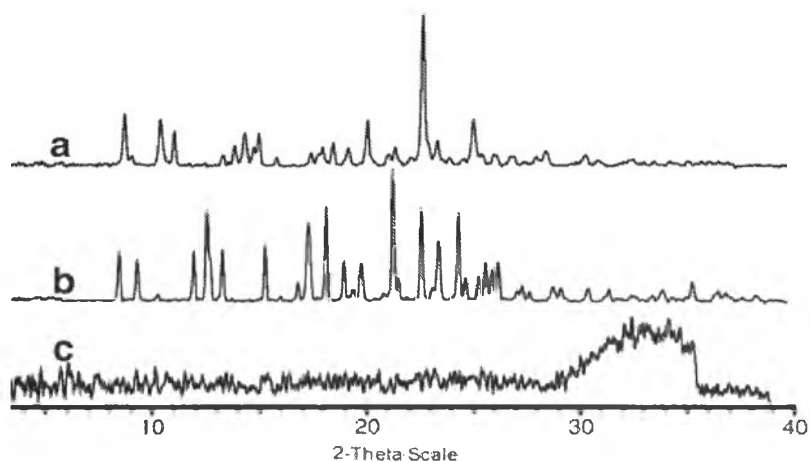


Figure 5 PXR D patterns of clopidogrel bisulfate polymorph Form I (a) polymorph Form II (b) amorphous form (c) (11)

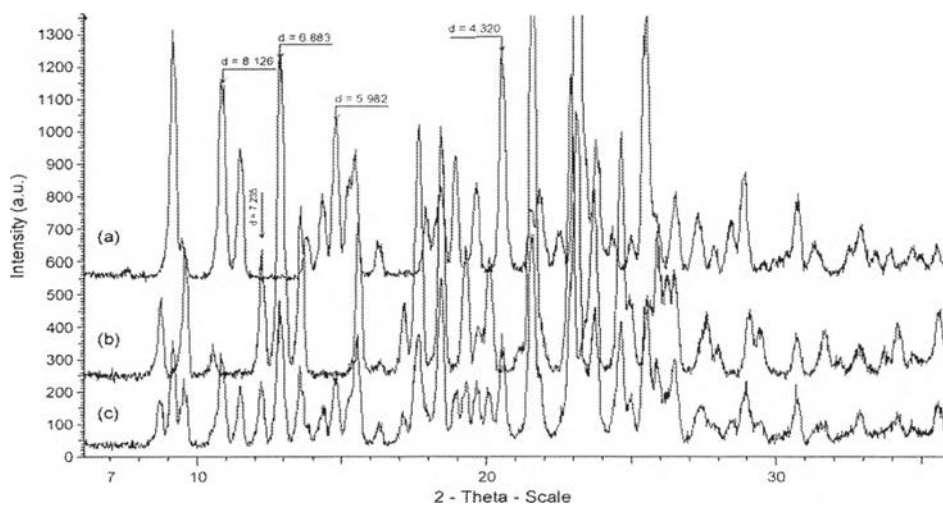


Figure 6 PXR D patterns of pure clopidogrel bisulfate polymorph Form I (a) pure polymorph Form II (b) mixture of two polymorphs Forms (c) (12)



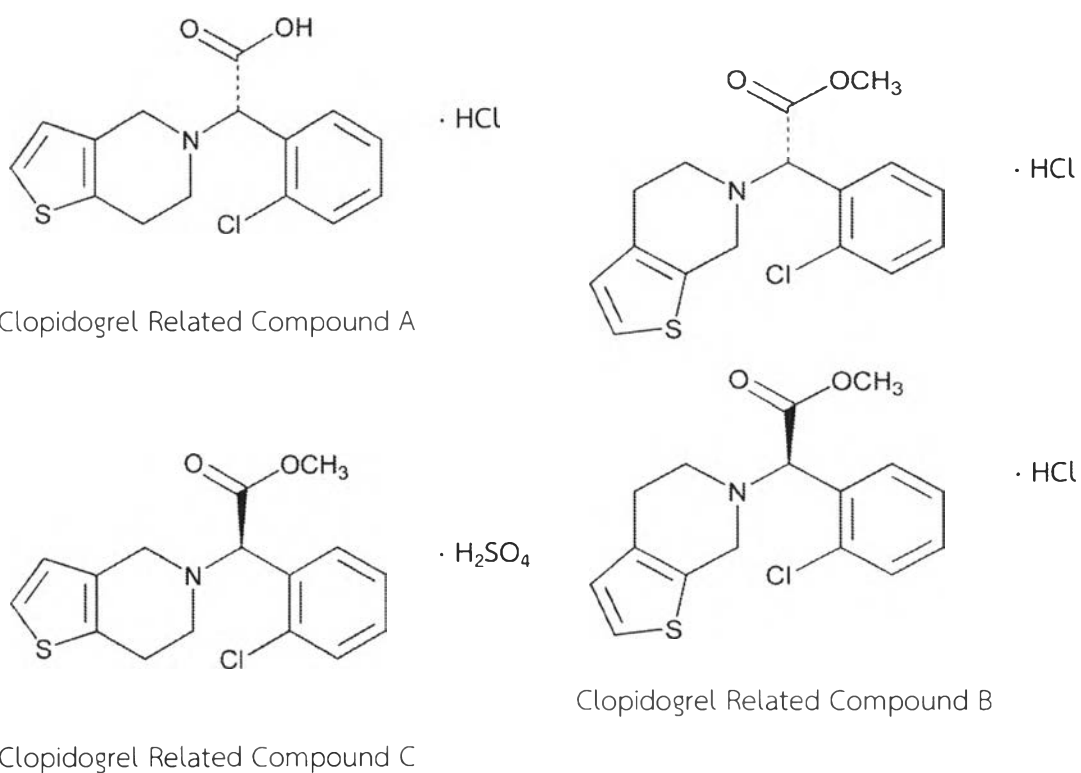


Figure 7 A chemical structure of clopidogrel related compounds (13)

There are 4 impurities of clopidogrel bisulfate have been already indentified and reported in the literature and the United States Pharmacopoeia (USP). These impurities consist of clopidogrel related compound A, positional stereo isomers of clopidogrel named as clopidogrel related compounds B1 and B2 and a chiral isomer of clopidogrel named as clopidogrel related compound C (Figure 7) (13, 14)

The United States patent number US 7,872,019 B2 exhibits topic about polymorphs and amorphous form of (s)-(+)-clopidogrel bisulfate. This patent reported that amorphous of (s)-(+)-clopidogrel bisulfate can be prepared by any suitable process. Amorphous drug substance of the present invention can be precipitated from solution or obtained from melt of compound by carrying out the solidification so as to avoid the thermodynamically crystallization process. Various processes



employed to obtain the amorphous (s)-(+)-clopidogrel bisulfate such as solidification of the melt, spray drying, freeze drying, reduction of the particle size, lyophilization, removal of solvent from solvate or hydrates, rapid freezing, milling, grinding, co-grinding and anti-solvents. Characterization of amorphous sample can be characterized by physical characteristics, melting point, powder X-ray diffraction pattern (PXRD), differential scanning calorimetry (DSC), thermogravimetric analysis (TGA), diffused reflection IR absorption and solid-state nuclear magnetic resonance spectrum (NMR) (15).

2. POLYAMORPHISM

Controversy about the presentation of “apparent” or “true” polyamorphism is an occasion for scientists to explore a lot of basics and practical features related to the amorphous state. Polyamorphism is the ability of a substance to existence in several different amorphous modifications. Polyamorphism’s definition is similar to the polymorphism of crystalline substances. Actually, it is interesting and challenging to verify the nature and origin of different physical, kinetic or thermal behaviors of two amorphous solids generated by different methods. This knowledge may create new concepts for the optimization of stabilization and manufacturing processes. For example, one substance can be prepared using various suitable procedures. Two amorphous samples of the same substance prepared by different methods show various molecular arrangements. Amorphous crystallinity of all amorphous samples should have value equal 0 but conventional tools cannot be used to evaluate the different samples generated by various methods. Therefore, the new technology is providing assess to help develop new instrument for evaluate them. These two amorphous solids can be concerned that they exhibit polyamorphous solids (16).



The occurrence of various amorphous structures can be considered from many opinions including the existence of specific physical, kinetic and thermal behaviors of separate molecular arrangements and of distinct energetic and thermodynamic properties. Polyamorphism also refers to the possible characterization and observation of solid-solid transitions finding between various amorphous solids. Polyamorphism may be imply the present of two glassy state (glassy forms) of the same substance which can be distinguished by their appearance and fragility. One of the glassy form is a low density of strong glass former but another form is a high density of fragile glass former (16).

3. PREPARATION OF AMORPHOUS SAMPLE

Amorphous solids are classified as non-crystalline solids that have a special status. These amorphous solids may be classified as a type of polymorph depending on the definition of polymorph. A long-range order referring simultaneous conformational, rotational and translational orders in the particles is a fundamental theory about separation between amorphous and crystalline solids. The single molecular unit is assumed that is repeated molecule according to a three-dimensional pattern along crystallographic directions in a crystal lattice. The relative location and orientation can be accurately explained about the interactions between neighboring components at the molecular level. Usually, the crystal packing of crystalline molecule plays a high density arrangement lead to a minimal molar volume. On the other hand, the absence of conformational, rotational and translational order in amorphous phases can be attributed to a random spread in the relative location and orientation of bordering molecule units. This orientation is implying to the molar volume that can be approximately calculate distance of the



probability of finding one molecule from another molecule. In conclusion, a short-range or local order exhibits existence of amorphous solids (16).

Amorphous or partially amorphous sample can be found by sample prepared at various conditions or different circumstances. For example, an amorphous sample can be generated by using unsuitable crystallization circumstance. Moreover, a in-processing procedure such as compression, desolvation, drying or milling can create different amorphous solids. Furthermore, an amorphous sample may be generated by enhance some of the biological or physical properties of the substance (16).

FROM A LIQUID PHASE: QUENCH COOLING

This method is the most normal process for generating glassy solids which is also called vitrification method. It comprises melting process at the temperature is above melting temperature (T_m) and must not chemical decomposition occurs during the melting (molten solution) and quench cooling process at the below its glass transition temperature (T_g) by without crystal lattice (crystallization process). In the melting step is carried out under nitrogen gas for avoid chemical decomposition. It is suitable to approach a quench cooling step using liquid nitrogen substances from above T_m within a few seconds. The viscosity of the glassy state substances is usually high at below T_g and exhibits the frozen liquid as a brittle glass when encounters with liquid nitrogen. The reduction of thermal motions and molecular motility from the liquid to a syrup or from a syrup to brittle glass can be observed by increasing viscoelasticity and a rubbery or malleable state characteristic of the supercooled liquid (16).



The cooling rate used to generate a glassy state of substance relies on the tendency of each compound to crystallization processes which is partially manipulated by the nucleation ability or by the conformational diversity existing in the liquid phase (16).

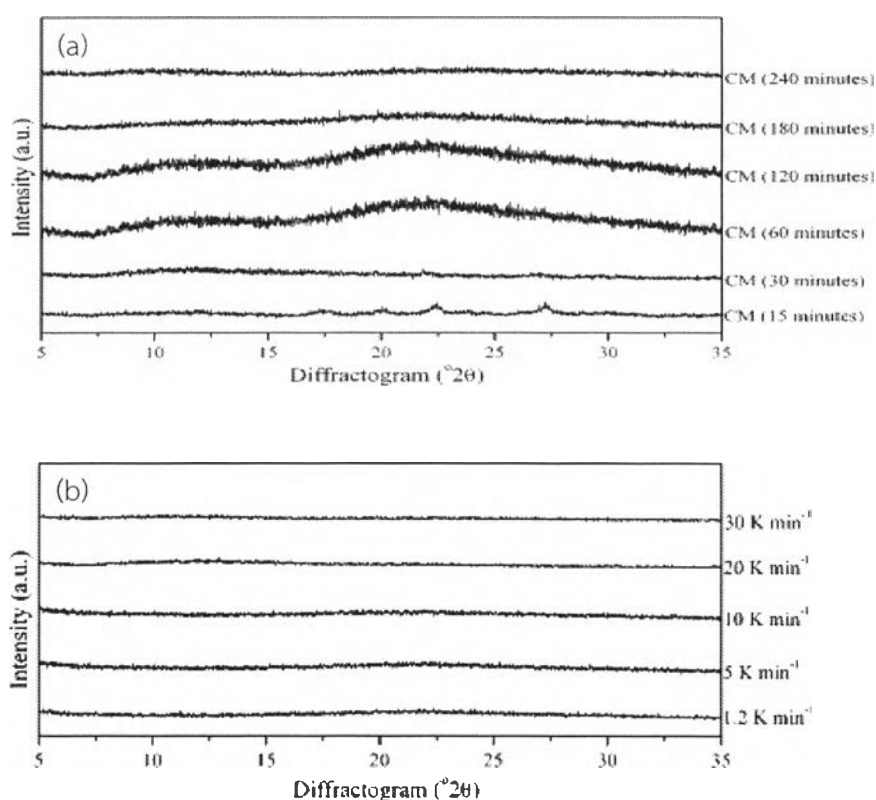


Figure 8 PXR D patterns of freshly amorphous samples of indomethacin generated by cryo-milling (a) melting and quench cooling (b) (17)

Karmwar et al. report that two amorphous indomethacin generated by cryo-milling and melting and quench cooling. These results are shown in Figure 8a and 8b. Figure 8a shows PXR D pattern of freshly amorphous samples generated by cryo-milling for various milling time. Figure 8b exhibits PXR D pattern of freshly amorphous samples generated by melting and quench cooling for various cooling rates. Both



amorphous indomethacin generated by two different procedures do not exhibit any other characteristic peaks (the lack of PXRD peaks) different to starting material (17).

FORM A SOLUTION: RAPID PRECIPITATION

Rapid precipitation can be prepared by very high supersaturated solution. Rapid precipitation processes may induce the formation of extremely low crystallinity solids or truly amorphous which are confirmed by the existence of a glass transition. Amorphous samples generated by rapid precipitation found that these samples are results from a swift change in pH or from the anti-solvents method (16).

Kim et al. exhibit the preparation of amorphous atorvastatin calcium generated by supercritical antisolvent (SAS) process. This result is shown in Figure 9. The PXRD patterns of unprocessed drug (atorvastatin calcium RM) show high intensity characteristic peaks at 9.12° , 9.44° , 10.23° , 10.54° , 11.82° , 12.16° , 16.97° , 19.45° , 21.59° , 22.62° , 23.22° and 23.68° 2θ . On the contrary, PXRD patterns of atorvastatin calcium after SAS process with various condition are not observed any characteristic peak (18).

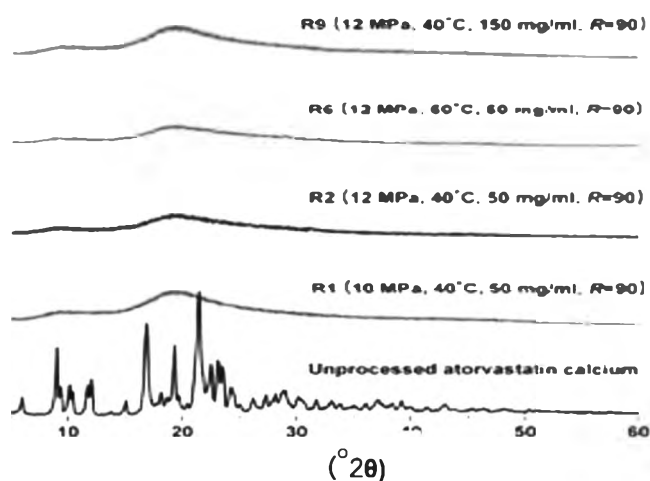


Figure 9 PXRD patterns of atorvastatin calcium before and after SAS process (18)

FROM A FROZEN SOLUTION: FREEZE DRYING (LYOPHILIZATION)

There are three successive steps of lyophilization consisting of freezing, primary drying and secondary drying. The freezing process of the solution usually soluble prepared by water but organic solvents, such as methanol, ethanol or isopropanol, can be a little bit added. This process should operate at below the eutectic constant temperature between the two constituents until the frozen substance. The primary drying process is operated under predetermine steps of low temperature and under constant low pressure condition by relying on the principle of sublimation of the frozen water or vaporization of the organic solvent. The secondary drying process involves removal of residual water or solvent that do not freeze (unfrozen molecule) by control temperature higher than ambient temperature at same pressure used in primary drying process. The nucleation or crystallization process can be avoided when the freezing process is rapidly occur using liquid nitrogen. The secondary drying step is the critical step because the presence of residual solvent lead to the crystallization process if the temperature is high enough (16).

Pralhad et al. studied the differentiate of pure quercetin (QURC), freeze dried QURC and mixture between APIs and β -cyclodextrin (β CD) using DSC, FT-IR, PXRD and SEM analysis. PXRD patterns of various samples are shown in Figure 10. The PXRD pattern of QURC powder shows characteristic peaks at 12.48° , 15.86° , 23.88° and 24.88° 2θ (Figure 10a). On the contrary, PXRD pattern of amorphous sample prepared by freeze drying exhibits characteristic only large diffraction peaks (Figure 10d) (19).



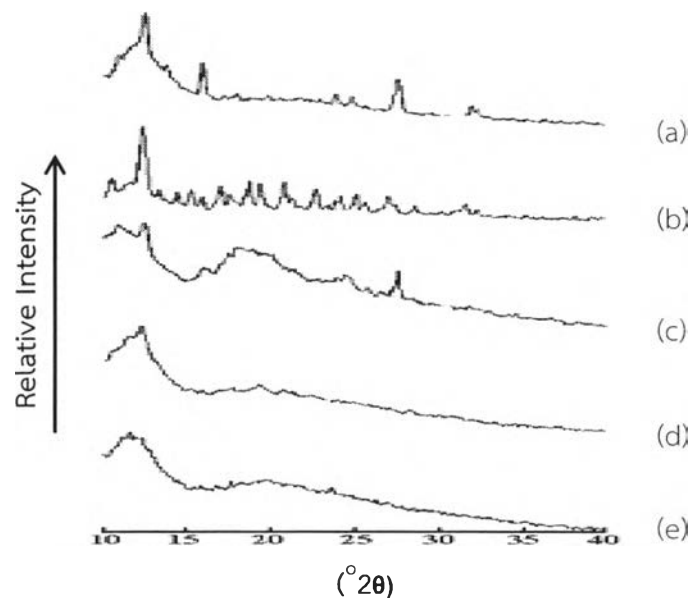


Figure 10 XRD patterns of QURC (a) QURC- β CD physical mixture (b) QURC-HP β CD physical mixture (c) freeze dried QURC- β CD (d) freeze dried QURC-HP β CD (e) (19)

FROM AN ATOMIZED SOLUTION: SPRAY DRYING

Spray drying method is suddenly drying process using a suitable solution or suspension which expose to high temperature at atmosphere. Drying process occur within second time when the liquid phase is spray from atomizer. The small atomizes have a maximal surface area and immediately expose to the drying gas. When spray drying method compare with freeze drying method, two methods give a similar glassy solids but a major difference between two methods is characteristic samples obtained by spray drying method having uniform spherical particles of desired size lead to good flow properties. On the contrary, freeze drying method creates irregular particles sizes. Prepared amorphous or glassy solids should be stored in low temperature and low humidity condition and protect from light because of low physical stability and conversion of amorphous to crystallize form of prepared sample (16).



Ohta et al. study the differences between two amorphous forms of spray dried cefditoren pivoxil prepared by various procedures. Amorphous samples generated by spray drying method which vary inlet air temperatures of 40°C and 100°C, called as SD-A and SD-B, respectively. PXRD patterns of different samples results are shown in Figure 11. Both of the initial prepared samples show only halo patterns indicated that both of the initial prepared samples are amorphous form of cefditoren pivoxil. Moreover, the PXRD pattern of SD-A sample shows PXRD peaks after four weeks storage due to there are crystallization process formation. On the other hand, the PXRD patterns of SD-B sample shows only halo pattern even though it is stored for eight weeks (20).

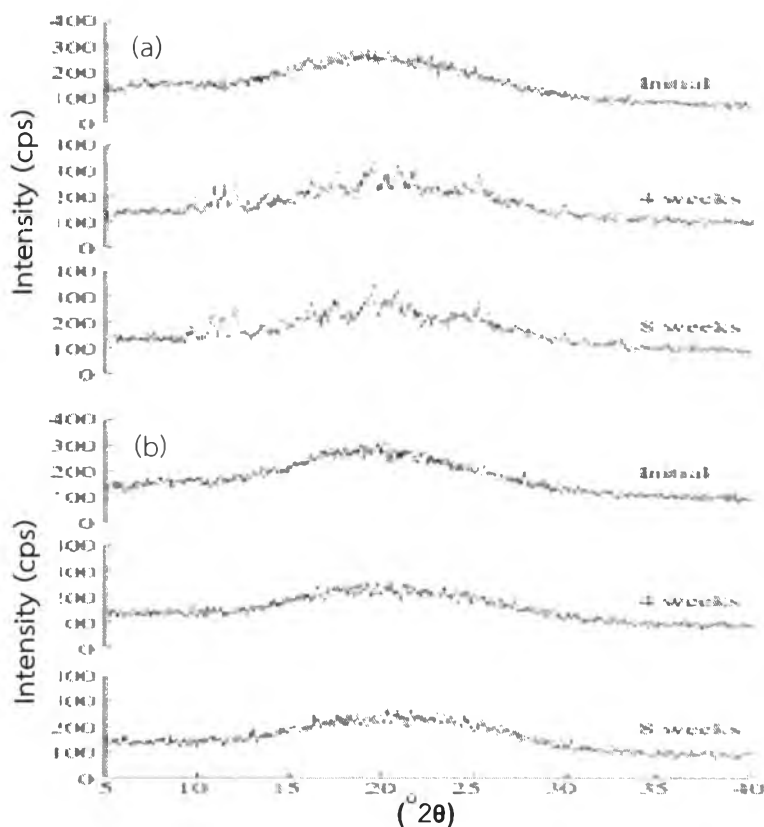


Figure 11 PXRD patterns of spray dried cefditoren pivoxil stored at 60°C and 81%RH using inlet air temperatures of 40°C (a) 100°C (b) (20)



FROM A CRYSTALLINE PHASE: GRINDING AND MILLING

Reduction of particle size is a one of the important process that used to often during the production of pharmaceutical industry. This process is used to reduce sizes at the first step until the final step of manufacturing process and research and development study. Reduction of particle size process such as grinding or milling can be used to study non-crystalline solids and used to study influence of solid-state properties and behaviors of amorphous solids. There is a difficulty that separate these solids obtained from reduction process that is the unclear distinction between microcrystalline forms and true amorphous solids. Microcrystalline forms present small crystalline particles which have particle size below or equal to 100 Å. On the other hand, true amorphous solids present the structure obtained from a frozen liquid and shapeless (16).

The bioavailability of drug substances depend on many their properties such as solubility, disintegration time, dissolution rate and partition coefficient etc. Prepared amorphous form is a one of the processes of the pharmaceutical industry and researcher to improve water solubility and increase dissolution rate. Various techniques are used to prepare amorphous solids in pharmaceutical systems such as anti-solvent, melting and quench cooling, rapid precipitation from solution or suspension (spray drying and freeze drying) and mechanical activation (milling). Karmwar et al. investigate the different amorphous indomethacin solids generated by various techniques consisting of cryo-milling (CM), ball milling (BM), spray drying (SD) and quench cooling (QC) (21). PXRD patterns of different samples are shown in Figure 12.



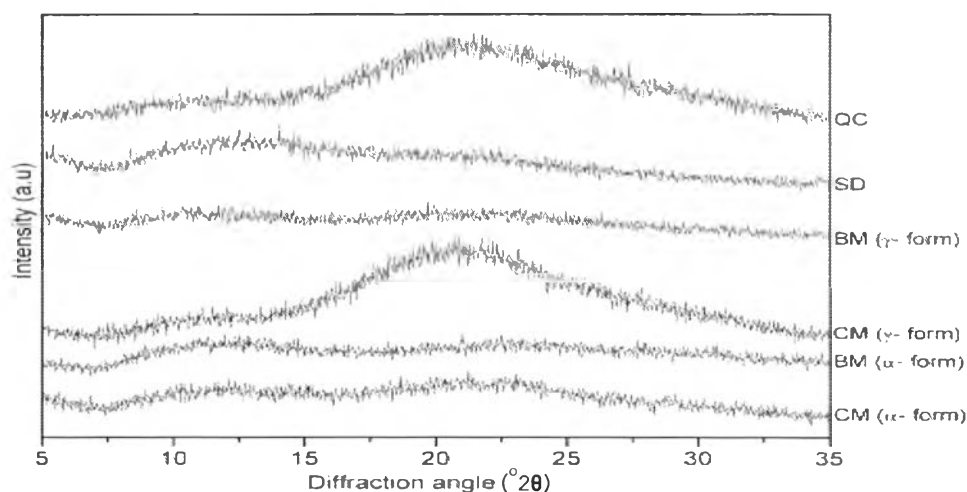


Figure 12 PXRD patterns of freshly amorphous form of indomethacin generated by different techniques: cryo-milling (CM), ball milling (BM), spray drying (SD), quench cooling (QC) (21)

Figure 12 exhibits the PXRD patterns of freshly amorphous solids of indomethacin generated by different techniques. All PXRD patterns of freshly prepared amorphous solids show only halo pattern or complete absence of diffraction peaks indicated that all initial prepared samples are completely amorphous form. However, all PXRD patterns obtained from freshly amorphous solids are found that having different shape lead to structural variations in the molecule between various amorphous samples. The diffractogram patterns of the QC and CM (γ -form) have maximum intensity at approximately $21^\circ 2\theta$. On the other hand, the diffractogram patterns of the BM (γ -form), BM (α -form) and CM (α -form) have closely position and intensity while slightly different shape. In 2009, Zhang et al. reported about influence of amorphous simvastatin generated by various procedures impacting on the physical and chemical stability. PXRD patterns of

different samples are shown in Figure 13. In addition, this study observed effect of particle size to recrystallization is shown in Figure 14 (22).

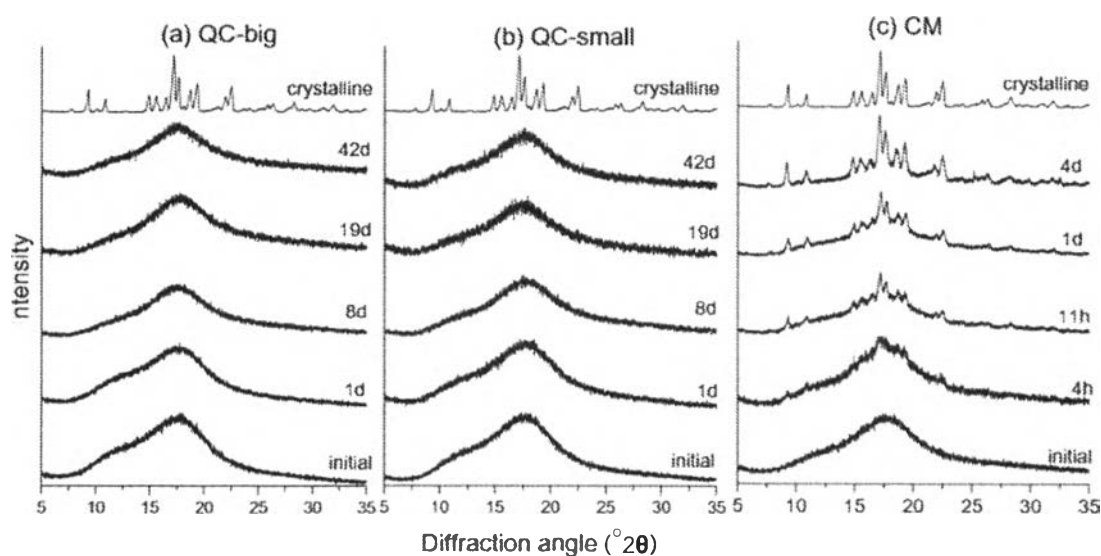


Figure 13 PXR D patterns of amorphous simvastatin (stored at 25°C) prepared by quench cooling big (QC-big) (a) quench cooling small (QC-small) (b) cryo-milling (CM) (c) (22)

Figure 13 shows PXR D patterns of amorphous simvastatin generated by various procedures and stored at temperature of 25°C. All three samples prepared at day 0 show halo pattern and do not exhibit any diffraction peaks. These results indicated that simvastatin samples prepared at day 0 are amorphous form. CM sample prepared and stored at 25°C shows recrystallization peaks within 4 hours (Figure 13c). On the contrary, QC-big (Figure 13a) and QC-small (Figure 13b) samples remain amorphous form after stored for 42 days. Figure 14 indicate PXR D patterns of amorphous simvastatin generated by various procedures and stored at temperature of 55°C. The QC-big sample remains absolutely amorphous form which is observed from lacking any crystallization peak after stored for 1 day (Figure 14a). On the other

hand, QC-small (Figure 14b) and CM (Figure 14c) samples have already started to recrystallization after stored for 1 day and 4 hours, respectively. These results exhibit that increasing of temperature (from 25°C to 55°C) has be impact on recrystallization of amorphous samples (22).

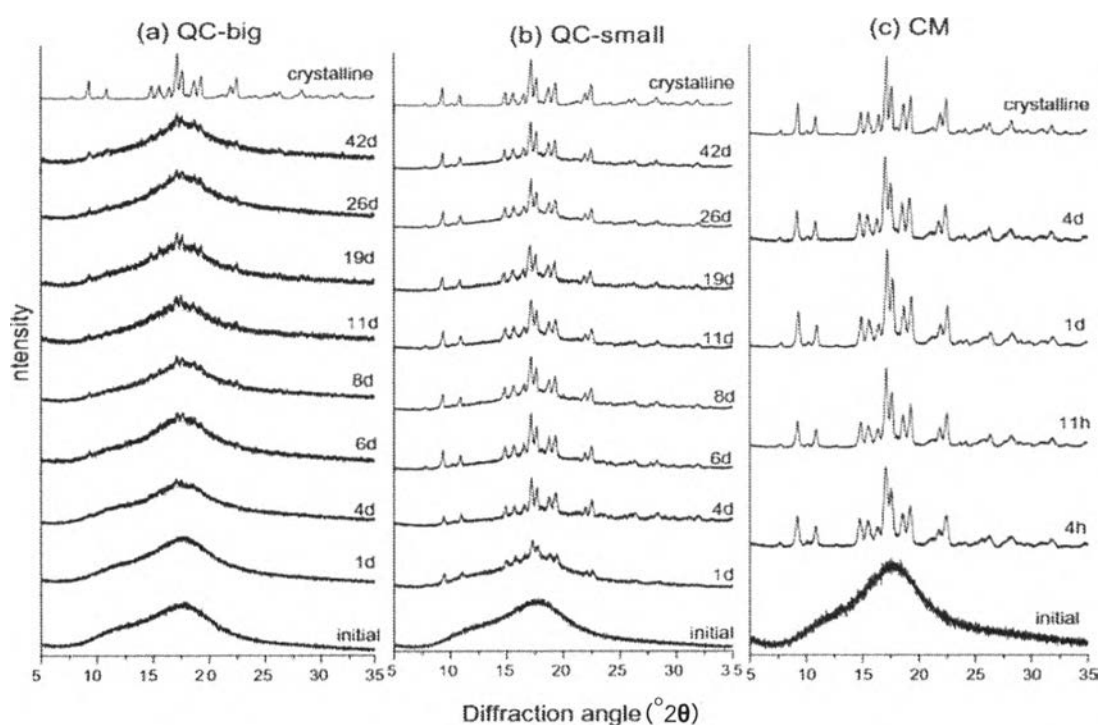


Figure 14 PXR D patterns of amorphous simvastatin (stored at 55°C) prepared by QC-big (a) QC-small (b) CM (c) (22)

4. SOLID-STATE CHARACTERIZATION

The solid-state characterization of active pharmaceutical ingredients (APIs) is very important knowledge in drug development process owing to their implications about the biopharmaceutical and physicochemical properties of these substances (1). The arrangement of many same single molecules that is the smallest repeating unit of a crystal is called the unit cell. The crystalline organic solids are the

molecules ordered or packed in a specific arrangement. In addition, the polymorph is defined that is the multiple crystal forms consisting of same molecular formula. On the other hand, non-crystalline solid is called amorphous form is explained that is the molecules which are not ordered or packed in a specific arrangement (random arrangement) (23). The amorphous structure is usually described with short-range molecular arrangement (lacking long-range order) similar to the crystalline structure (24). The amorphous solid that lack any long range orientational-translational symmetry within the molecules effect on any physicochemical and biopharmaceutical properties of the drug substances. Figure 15 exhibits the immediate circumstance of a molecule (m) in an amorphous solid. These molecular arrangement may not be significantly different from crystalline solid due to both of them have same number and distance to the nearest neighbors (24).

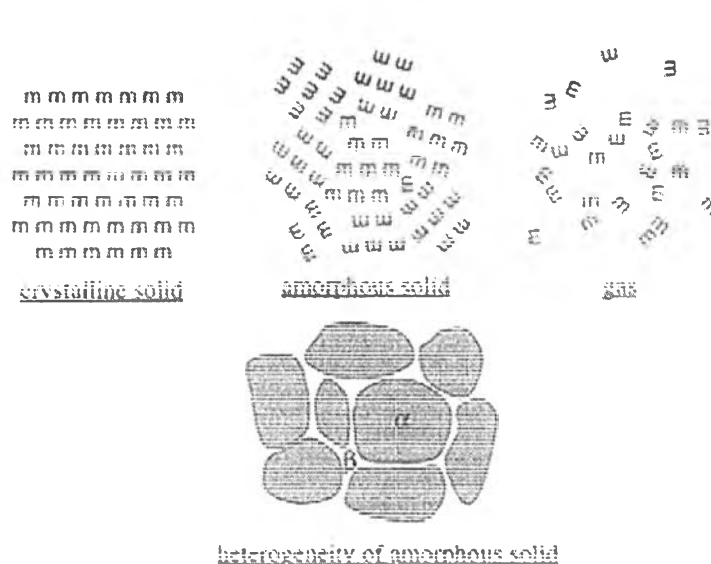


Figure 15 Schematic representation of the structure of crystalline solid, amorphous solid and gas (24)

There are many techniques used to evaluate the solid-state properties of drug substances and used to characterize and control amorphous form of drug substance such as polarized light microscopy, differential scanning calorimetry (DSC), thermogravimetric analysis (TGA), infrared (IR), Near-infrared (Near-IR) and Raman spectroscopy. These techniques are excellent methods for obtaining structural information and have been regularly utilized to discriminate polymorphous form. Zupančič reported that clopidogrel acid and clopidogrel salts can be distinguished between various samples using Fourier transform infrared spectroscopy (FT-IR), power X-ray diffraction (PXRD), ^{13}C and ^1H nuclear magnetic resonance (NMR) spectroscopy and dynamic vapor sorption (DVS) analysis (9).

4.1. POWDER X-RAY DIFFRACTOMETRY

Power X-ray diffractometry (PXRD) is the primary tool for analysis and for the study polymorphic transformation. PXRD is a one of the most powerful experimental equipment to study electronic structures. PXRD spectra are responsive to the chemical environments changes of elements in molecules and solids. Furthermore, this method is an effective method for distinguish solid phases having different internal structure. Moreover, this method is simple and does not require large sample. In addition, this method can be apply to any powder sample and do not sample preparation procedure.

The consideration into use power X-ray diffractometry (PXRD) is the situation different between truly amorphous solids and microcrystalline states. Reduction process (mechanical milling or grinding) of crystalline solids may remove all traces of crystallinity investigated by using PXRD (show only halo pattern) but the resulting



material is not amorphous solids due to particles size obtained have diameter below or equal to 100 \AA . Eventhough micronization process should ultimately lead to an amorphous solid. The existence of microcrystalline state (very small crystals solids) cannot be detect by PXRD apparatus due to the limitation of this apparatus. In this case, DSC analysis used to investigate for separate between amorphous solids and microcrystalline states depended on the presence or absence of glass transition in DSC chromatogram (24).

FUNDAMENTAL PRINCIPLES OF X-RAYS DIFFRACTION

The X-rays are short-wavelength electromagnetic radiation generated by bombarding matter with high energy particles such as electrons or protons or X-ray photons. When an atom is bombarded in this manner, an electron is ejected from one of the inner shells of the atom, leaving a hole or vacancy. This vacancy is immediately fulfilled by another electron in the atom from a higher energy shell, giving off an X-ray in the transition to conserve energy. The wavelength range of conventional X-rays spectroscopy is about 0.1 \AA to 200 \AA . However, usually used to the region of about 0.7 \AA to 2 \AA for analysis. When the X-rays passed through a sample, the electric vector of the radiation will be contacts with the electrons in the atoms of the substance to produce scattering into many specific directions. There are two types (constructive and destructive) of interference occur among the scattered rays when the X-rays are scattered by the ordered environment in a crystal. The scattering of sample produces constructive interference of X-rays by the atoms of crystal called the diffraction pattern which shows information about the structure of the crystal (25).



Figure 16 shows a PXRD consisted of an X-ray source which normally an X-ray tube, a sample stage or sample holder, a detector and a way to change angle θ of X-ray beam. In the beginning, the X-ray beam will be focused on the sample which put on the sample holder at some angle θ called angle of incidence, whereas the detector located in opposite of X-ray source indicate the intensity of the X-ray beam which it obtains from the source path at angle 2θ called angle of scattering. The angle of incidence can be more increased over time, whereas the angle of scattering always remains angle 2θ above the source path (26).

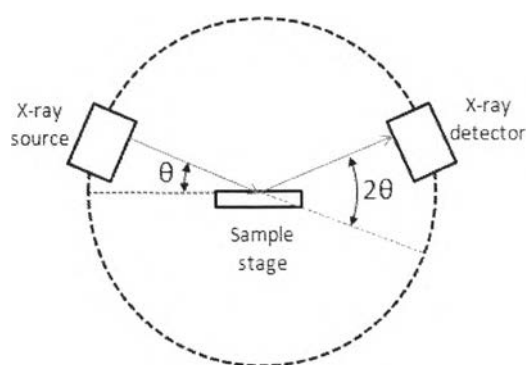


Figure 16 Angle of incidence and angle of scattering from PXRD instrument (26)

Bragg's Law (Equation 1) relates the wavelength of electromagnetic radiation or subatomic particle waves produced the diffraction angle comparable to the lattice spacing in a crystalline sample. Figure 17 shows an X-ray beam (A) passing into a crystal surface at some angle (θ) called the angle of incidence, the part of the beam is scattered (B) by the layer of atoms at the surface. The scattering angle is value same angle obtained from X-ray beam collides with the surface called the angle of scattering (the angle of incidence = the angle of scattering). The non-scattered part of the beam (the second incidence beam, C) penetrate into the second layer of the

atoms where again a fraction is scattered (D) at the second layer, and the remainder passes on to the next layer continue and so on (27).

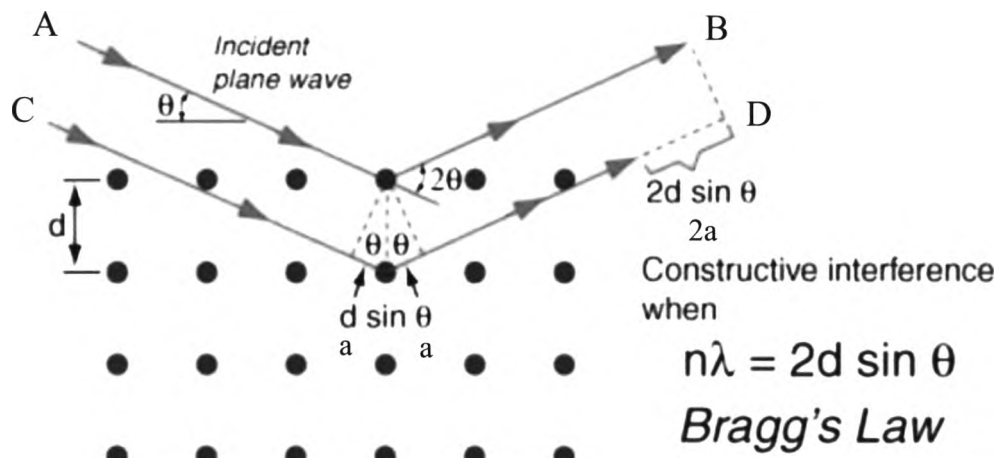


Figure 17 Theory of Bragg's law (27)

Figure 17 exhibits a distance of CD (second beam) line which has a distance farther than AB (first beam) line equal to $a+b$, when a is ED distance and b is DE distance but ED distance equal to DE distance (when $a=b$; $a+b = 2a$). If two beams are continuous parallel moving. This distance ($2a$) must be equal to an integral (n) of the wavelengths ($n\lambda$). In case of distance ($2a$) is equal with $n\lambda$, the constructive interference will be able to occur. On the contrary, distance ($2a$) is not equal to $n\lambda$, the destructive interference will be occurred and the scattering beam will not strong and cannot enter into the crystal. Therefore, distance ($2a$) must be equal value to $n\lambda$ for create constructive interference as follows

$$n\lambda = 2a$$



From trigonometry, we can use to predict the distance ED (a) and DE (b) by relation between the spacing (d) within the atomic planes and angle θ

By:
$$\sin \theta = a/d \quad \text{or} \quad a = d \sin \theta$$

Thus :
$$n\lambda = 2d \sin \theta \quad (\text{Bragg's Law Equation}) \quad (\text{Equation 1})$$

When: d = The distance between the atomic planes in the crystal lattice

θ = The X-ray incidence angle or the X-ray scattering angle

λ = Wavelength of the X-rays beams

n = Integer order of the diffraction pattern

When n is unity, the diffracted radiation is called first order. Higher orders of diffracted radiation fall off in intensity. Equation ($n\lambda = 2d \sin\theta$) is known as Bragg's law equation. For this equation, X-rays beam given the wavelength any diffraction will be observed from only certain values of θ (determined by d). Therefore, these θ values can be explained by rotation the crystal and measuring the angle of scattering (diffracted X-rays beam) which should be equal to the angle of incidence. The d spacing between atomic planes can be calculated by this equation. On the other hand, if the d spacing of a crystal is known, the angle of incidence and the angle of scattering (diffracted X-rays beam) can be calculated.

4.2. DIFFERENTIAL SCANNING CALORIMETRY

Differential scanning calorimetry (DSC) is the most often used thermal analysis method. The advantages of this method consist of its speed, accuracy, precision, simplicity, availability and no need sample preparation. On the other hand, the most



disadvantage of this method is high cost of consumer product (pan) and instrument and maintenance. DSC instrument chamber consists of a sample and a reference placed in sample and a reference holders, respectively. The higher temperature is obtained from heater either ramp the temperature at a specified constant rate or hold at constant one temperature until finished experiment called isothermal DSC. In case of the temperature of both the sample and reference are increased at a constant rate. The final result interprets information obtained from the difference between the sample and the reference of heat flow.

INSTRUMENTATION

There are three different types of DSC apparatuses composed of power-compensated DSC, heat-flux DSC and modulated DSC. Results from all DSC types will be created a DSC thermogram which is a plot between heat flow or power versus temperature (25).

POWER-COMPENSATED DSC INSTRUMENTS

The concept of power-compensated DSC is the equal heat measured between sample and reference probe. The temperature of the sample is under control condition equal to the temperature of the reference. The measured heat is compensated with electric energy by varying the power input to the two furnaces (increasing or decreasing an adjustable Joule's heat).



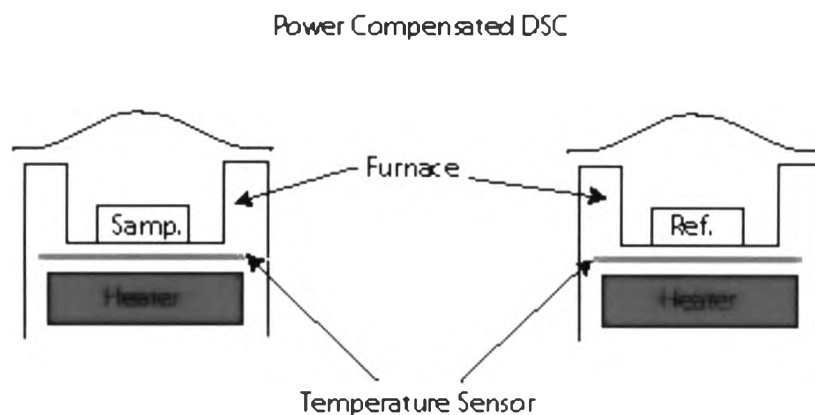


Figure 18 A diagram of a power-compensated DSC instrument (28)

Figure 18 shows a diagram of a power-compensated DSC instrument consisting of two sample holders (one sample and one reference), furnace (heating unit) and temperature sensor. Two heating units are independently controlled. These heating units are quite small parts (microfurnaces) which have outstanding capacity such as rapid rates of increasing heat, decreasing cool and equilibration. The heating units are embedded in a large thermostat (temperature-controlled heat) block. The reference and sample holders contain platinum resistance thermometers to continuously monitor the temperature of the both holders. Both of the sample and the reference are operated at the programmed temperature by applying vary power to the reference and sample heaters in order to adjust between both temperature. The instrument measures the different power used to maintain equilibrium between the reference and sample the at the same temperature (25).

HEAT-FLUX DSC INSTRUMENTS

The concept of heat-flux DSC is the different temperature measured by insertion of heat flow at a constant rate into the reference and sample. Figure 19 shows a diagram of a heat-flux DSC instrument. Both of the reference and the



sample are increased temperature using a single heating unit. Heat flows pass into both the reference and the sample material through an electrically metallic block with high thermal conductivity that ensures a good heat flows called constantan thermoelectric disk.

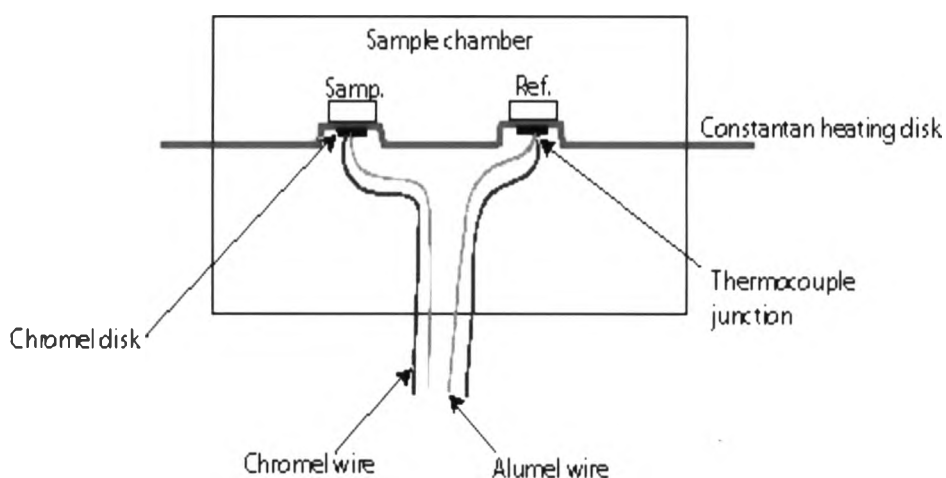


Figure 19 A diagram of a heat-flux DSC instrument (28)

Small aluminium reference and sample pans put on increased operation blocks on the constantan heating disk. Heat is carried through the disks and sent into the material same the two pans. The differential heat flow between reference and sample is observed by Chromel-constantan area thermocouples. This equipment is created by the connection between the constantan platform and Chromel disks which are embedded into the underside of the platforms. Each temperature pans is evaluated by the Chromel-alumel junction under the each disks. Therefore, the differential heat flow between both pans directly associated with the difference in the outputs of the two thermocouple junctions. (25).

MODULATED DSC INSTRUMENTS

The modulated DSC (MDSC) instruments consist of cell arrangement and heating unit similar to the heat-flux DSC apparatuses. A sinusoidal function of MDSC is imposed on the total temperature program to create a micro heating and cooling cycle. A sinusoidal modulation is overlaid on the conventional linear heating or cooling rate to produce the average sample temperature profile which continuously changes in a non-linear manner. The advantages of MDSC involve the resolution of the total heat flow measured. In conventional DSC the total heat flow is measured by one heat flow component, whereas in MDSC the two individual heat flow components are measured individually. In MDSC the overall signal using Fourier transform method is mathematically manipulated into two parts which consist of a reversing heat flow signal and a non-reversing heat flow signal. The reversing heat flow signal is associated with the heat capacity component of the thermogram. On the contrary, the non-reversing heat flow is related to kinetic processes. Step transitions such as the glass transition usually appear only in the reversing heat flow signal, whereas exothermic or endothermic thermograms may appear in both heat flow signals (25).

DSC DATA ANALYSIS

The software program in the modern DSC apparatuses is used to help the user in calculating onset temperature (melting points), peak temperature, end-set temperature, glass transition temperatures and heat capacity values. The temperatures of step transitions are usually determined as onset temperatures and melting point. Figure 20 indicates the onset temperature of any samples. The onset temperature is defined as the temperature point which a line tangent intersects with



the baseline and this tangent line is the slope of the transition. Moreover, the peak temperature is the maximum or minimum point of step transitions (29).

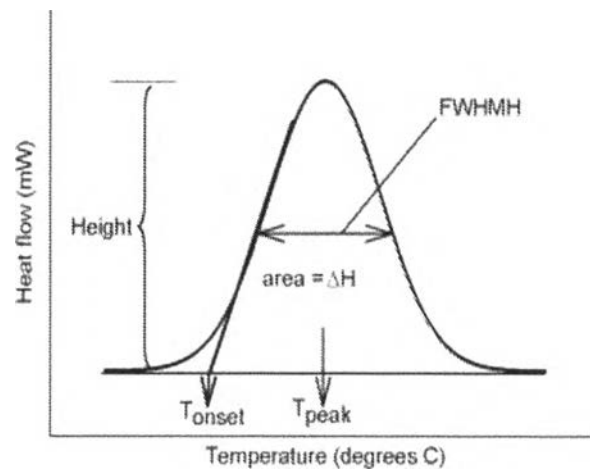


Figure 20 Determination of onset temperatures (29)

Furthermore, the glass transition temperature is related to the change in heat capacity from one transition state to another transition state. In case of increase temperature, the transition step will be change from glassy state to rubbery state. Therefore, the temperature at the border from the glassy state to the rubbery state is called its glass transition temperature which is generally indicated as T_g . The change in heat capacity is usually determined as the difference between the onset point and the end point of the transition. The enthalpy of crystallization, recrystallization or melting is determined by integrating the endothermic or exothermic peak corresponding to a give transition. Result from integration is area under the curve of the endothermic or exothermic peak.



4.3. THERMOGRAVIMETRIC ANALYSIS

The concept of thermogravimetric analysis (TGA) is the amount and rate of weight changes in a sample which is continuously recorded whereas the temperature of each experiment is increased. This device is used to provide more detailed chemical information through examination of the decomposition by products. A plot between mass or mass percentage and a function of time is named a TGA thermogram or a thermal decomposition curve.

INSTRUMENTATION

Figure 21 indicates a cross-section diagram of thermogravimetric analysis (TGA) instruments. This instrument consists of a thermobalance (sensitive microbalance), a furnace system (temperature system), a purge-gas switching system for providing and eliminating an inert or reactive gas and a computer system for device management, data acquisition and data processing. A purge-gas switching system and rate of increase temperature are a usually function applications which must be adjusted during an experiment called programmable furnace (25).

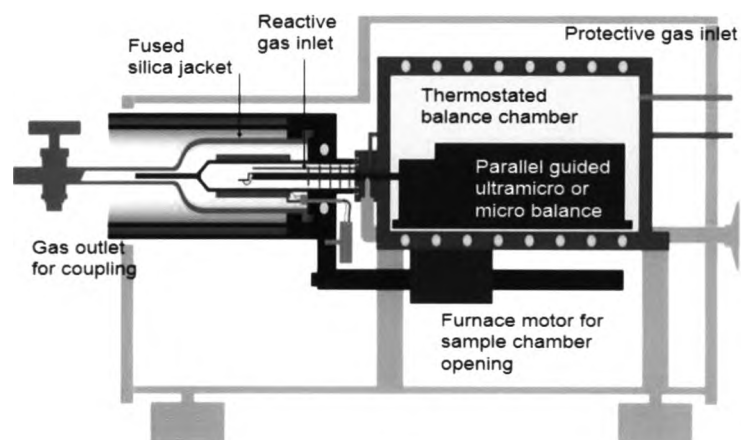


Figure 21 A diagram of thermogravimetric analysis (TGA) instrument (30)

THE THERMOBALANCE

The thermobalance is a type of the sensitive microbalance. The available designs of commercially different thermobalance are capacity of providing quantitative information about samples weight range from less than 1 mg to 100 g. The usually normal range of thermobalances is from 1 to 100 mg. A lot of the balances can be detected the weight changes as low as 0.1 μg . Eventhough the sample holder will be embedded into the surface of furnace, the microbalance arm must be isolated from the furnace. The weight change of sample is caused from a deviation of the beam which obstructs the light between a lamp and the one of two photodiodes. This imbalance results in the photodiode current is amplified and deliver to a coil which is installed between the poles of permanent magnet. The amplified photodiode current is measured and transformed into weight or weight loss information by the computerized data processing system (25).

THE FURNACE

Furnaces for TGA typically cover the range from ambient temperature to 1000°C but some samples want to use furnace for temperatures up to 1600°C. The heating rates can be usually decided from 0.1°C/min to 100°C/min but some samples can heat as rapidly as 200°C/min. The cooling system is installed outside the furnace and the insulation is needed to avoid heat transfer to the balance. The inert gas (nitrogen or argon) is often selected to eliminate heat of the furnace and prevent oxidation reaction of the sample. When the sample is heated through its Curie point, the magnetic mass is lost and the balance indicates an apparent loss in mass. The temperature accuracy and precision are better than 1°C and typically uncertainty $\pm 0.1^\circ\text{C}$ with the usually furnace, respectively. The most furnaces are



reduced temperature by the forced cooling air which can be reduced from 1000°C to 50°C in less than 20 minutes (25).

SAMPLE HOLDERS

Samples are usually contained in the sample pans created from platinum, aluminum or alumina materials. This material is most often used because of its inertness and ease of cleaning. The normal volumes range of sample pans is from 40 µL to more than 500 µL. Autosamplers are available as attachments for most TGA systems. All procedures can be automatically operated under software control (25).

TEMPERATURE CONTROL AND DATA PROCESSING

The ideal temperature is the actual temperature of the sample obtained from each experiment. This actual temperature of the sample can be received by immersing a small thermocouple directly in the sample. Some resulting from the thermocouple cannot immerse a small thermocouple into the sample. Therefore, the recorded real temperature is usually measured with a small thermocouple settled under closely possible to the sample pan. From this reason, the recorded temperature is generally used to substitute for the actual sample temperature (25).

The modern TGA systems utilize by automatically computerized temperature control principle. The computerized system will detect the difference between the temperature of the thermocouple and the temperature in order to adjust the voltage of the heater. In some systems, the heating element and the temperature sensor will be installed in the same thermocouple.



4.4. DYNAMIC VAPOR SORPTION

Dynamic Vapor Sorption (DVS) is used to evaluate the interaction of water vapor within solid materials. The plot of the equilibrium vapor content of a solid material compare to a series of step change (predetermined) in relative humidity (RH) which consists of sorption cycle (increasing RH step) and desorption cycle (decreasing RH step) at constant temperature called vapor sorption isotherms. The equilibrium mass values at each RH steps are apply to generate the sorption isotherm. Sorption and desorption isotherms can be evaluated gravimetrically by measuring the mass change of a sample with upper and lower change in RH, respectively.

INSTRUMENTATION

The DVS is significantly automated moisture sorption analysis. The DVS instrument operates in a closed system at controlled constant temperature and either ambient or controlled constant pressure. The sample is inserted in a sample pan of microbalance and exposed to a continuous flow of air or inert gas (N_2) of a series of step change (predetermined) in RH within instrument. This process will be operated until the mass change of sample has reached equilibrium at this step and then continue to next step as follows to predetermined RH. A DVS isotherm is created from the equilibrium mass value (moisture uptake) at each RH steps. Due to the mass change must stabilize at incremental each RH, therefore, the duration at each step of the experiment will depend on the nature of individual sample. The individual sample can be moisture uptake on the surface called surface adsorption which is typically relatively fast, whereas the surface absorption is moisture penetrating into the inside of the sample (16).



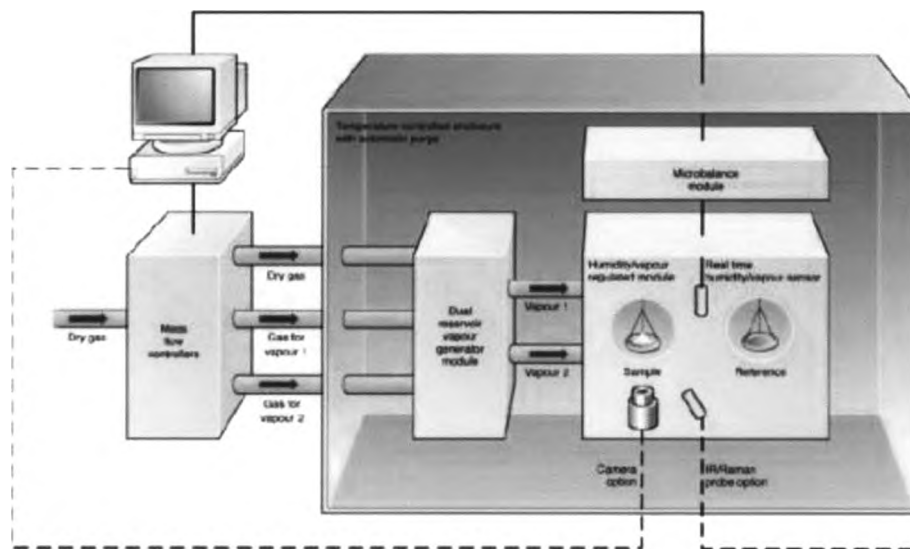


Figure 22 A cross section of the Dynamic Vapor Sorption (DVS) instrument (31)

Figure 22 shows a cross section of the Dynamic Vapor Sorption (DVS) instrument. This instrument is used to measure the moisture uptake and the loss of vapor gravimetrically depending on ability of microbalance which usually comprises a weight resolution at least $\pm 0.1 \mu\text{g}$. The vapor pressure covers around the sample created by dry carrier gas streams using electronic mass flow controllers. The DVS device has the unique competency to actively measure and control a wide range concentration of water or organic vapors (31).

4.5. POLARIZED LIGHT MICROSCOPE

The polarized light microscopy uses plane-polarized light in order to evaluate structures. Figure 23 shows a schematic diagram of the polarizing light microscope. This microscope is a type of compound light microscope which is adjusted by replacing one polarizing filter (the polarizer) below the rotating stage (under the specimen) and replacing another polarizing filter (the analyzer) after the objective lens (above the specimen). The vibration direction of the electromagnetic passed



polarizer is usually aligned called plane polarized light. Its plane of polarized light align from west to east, in other words, align from left to right when observed through the microscope. Moreover, the vibration direction of the analyzer is aligned 90 degree (perpendicular) with the polarizer.

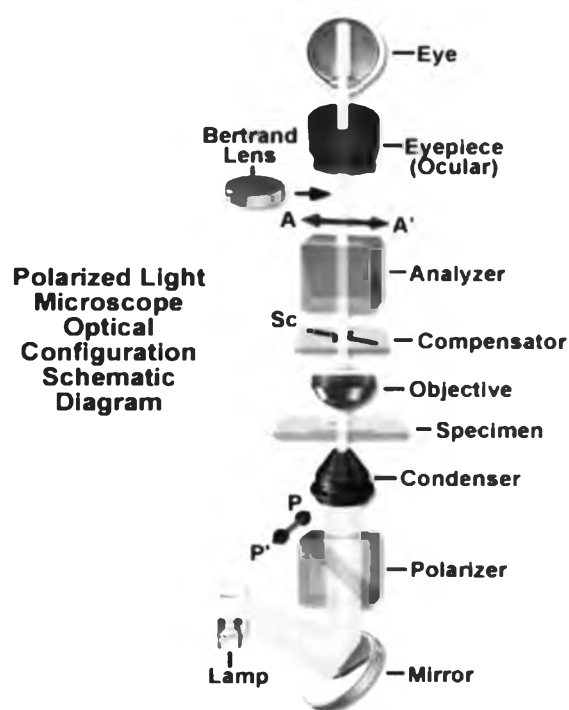


Figure 23 Schematic diagram of the polarizing light microscope (32)

The polarizer is usually embedded in the light path at all times and is settled between the specimen and the illuminator. The modern polarizer is typically incorporated into the condenser. The analyzer is designed in order to it can be inserted into the light path. The analyzer is usually placed between the objective and the ocular tube. Some microscope will permit the analyzer to be rotated associated with the polarizer. Therefore, specimens can be observed between uncrossed polarizers and analyzers using specialized compensator plates for characterizing optically active specimens.

4.6. RAMAN SPECTROSCOPY

Raman spectroscopy is one of the spectroscopic techniques for investigating drug substances. Spectroscopic techniques consisting of Raman spectroscopy, ultraviolet (UV) spectroscopy, infrared (IR) spectroscopy, near-infrared (near-IR) spectroscopy and microwave spectroscopy which are based on the interaction of each selected radiation. By the quantum theory, the energy of each radiation is directly proportional to its frequency ($E = h\nu$, where ν is frequency and h is the Planck's constant (6.626×10^{-34} J·s)) and can be explained to the effect on its molecule. For this reason, the high energetic radiation such as UV and visible promotes electronic transitions within molecule, while the low energetic radiation such as IR and microwave creates vibrational and rotational movements within molecule. Raman spectroscopy is classified as a type of vibrational spectroscopic technique similar to IR spectroscopy. Vibrational spectroscopy methods are very high important apparatus for the qualitative and quantitative analysis. Qualitative analysis is used to analyze in a part of identification and characterization of active pharmaceutical ingredients (APIs) because they provide fingerprint spectra pattern which are unique of individual compound. Moreover, it is widely used as a quality control tool in part of quality assurance for study on chemical identification or analyzing quantitatively drug substances. This method provides high sensitivity and selectivity against molecular compound that has crystalline structure within molecule. There are many vibrational spectroscopies used to investigate drug substances but Raman spectroscopy is a most famous and should be the method of choice because the Raman spectra obtained this technique produce a rich in information. In addition, the low wavenumber region of the Raman spectra is easily



to accessible by Raman spectroscopy. This region exhibits the most of the significant vibrational information (fingerprint region) on the solid state. The measurements in the 4000-2800 cm^{-1} (X-H stretching) and 1800-300 cm^{-1} (fingerprints) regions are usually considered as molecular structure fingerprints of analytes (33). The Raman scattering gives information about structural changes within molecule. There are many advantages for using Raman spectroscopy to study polymorphism in pharmaceuticals due to lack of sample preparation, the ability of small volume sampling, fingerprint capabilities, non-invasive measurements, shorten of run time, speed of data acquirement, quantitative analyses, on-line monitoring competencies, weak water interference, reproducibility, automated high-throughput analysis and the high sensitivity. The best important advantage of Raman spectroscopy more than IR spectroscopy is not interfere of water within sample. Furthermore, sodium chloride or other unstable employed as window materials can be replaced by glass or quartz cells for avoid inconvenience of working. The Raman spectra normally exhibit spectra bands that are characteristic of the specific molecular bonds in the individual sample. The band's intensity of Raman spectrum is corresponded to the concentration of the molecules and can be used to calculate for quantitative analysis. The information obtained from Raman spectra can be explained specific data for good specificity of qualitative analysis and for discrimination among similar materials. Moreover, the Raman technique is relatively inexpensive compare to power X-ray diffractometry (PXRD) or solid-state nuclear magnetic resonance spectroscopy (SSNMR). Therefore, the investigations in pharmaceutical compounds using Raman spectroscopy give highly knowledge about specificities of the vibrational spectroscopy and help to fulfill data received from PXRD measurements.



Eventhough, both of techniques IR and Raman are recognized with measuring related to molecular vibration and rotation energy changes but IR absorption energy involves a vibrational mode of the molecule in order to change in dipole moment or charge distribution. On the contrary, Raman scattering sorption energy involves a momentary distortion of the electrons distributed around a bond in a molecule. In the momentary distortion of the electrons, there are temporarily polarized in the molecule induce dipole moment in the atom. This situation creates relaxation and reemission energy given vibration mode which may different from IR activity. By the summary, vibrational activity in Raman spectra require a change in dipole moment, while IR spectra require a change in the polarizability of the molecule during the vibration. From these reasons, there are possible to receive spectra informations from a homo-nuclear molecule using Raman spectroscopy called Raman active. Wartewig et al. reported that the clear difference between Raman spectrum and IR absorption spectrum of benzene are shown in Figure 24. Both spectra transmitted strong degree of similarity because there are different origins of each processes. IR bands are correspond to polar functional groups, while Raman bands are correspond to non-polar functional groups (34).



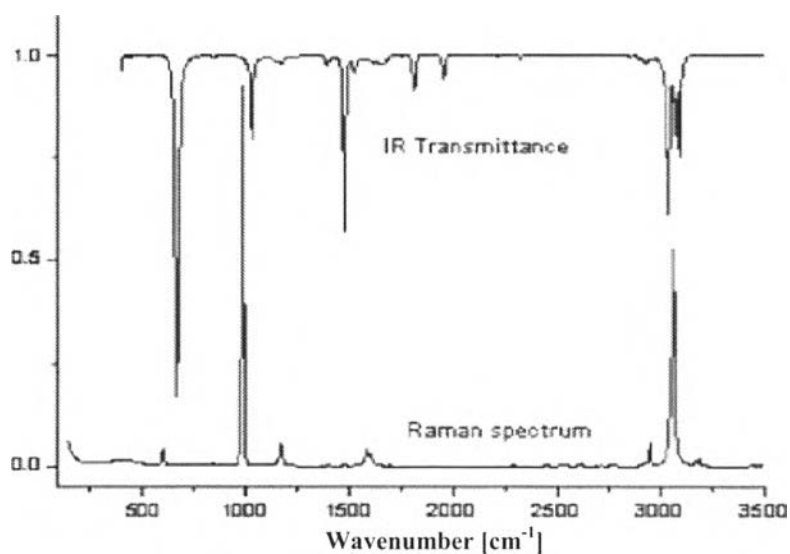


Figure 24 Comparison of the IR and Raman spectra of benzene (34)

Findlay et al. indicate the complementary nature of Raman and Infrared (IR) spectra of cyclohexane are shown in Figure 25. The CH_2 anti-symmetrical and symmetrical vibrations of the molecule exhibit characteristic peaks at 2933-2915 and 2897-2852 cm^{-1} which show existence of both IR and Raman activities. On the other hand, at wavenumber 1450 cm^{-1} exhibits a strong IR sorption peak of the CH_2 scissoring motion but show a only medium Raman peak. Moreover, at wavenumber 903 cm^{-1} finds a strong IR peak of the anti-symmetric ring stretching. On the contrary, at wavenumber 802 cm^{-1} presents a strong Raman peak of the ring breathing motion that arrange in chair form of cyclohexane (35).



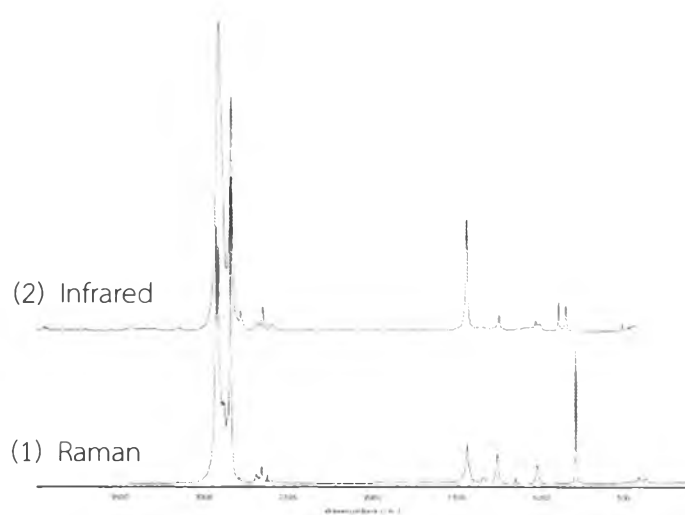


Figure 25 Infrared (IR) spectrum (1) and Raman spectrum (2) of cyclohexane (35)

Raman spectra show a detectable change in their arrangement due to crystal lattice change after dehydration. This reason causes Raman spectroscopy also operated as process analytical technology (PAT) because of its insensitive to aqueous solvents. Hausman et al. study on-line Raman spectrum of drying process in granulation step at the start (a) and of drying process in granulation step until 1% moisture at the end (b) shown in Figure 26. Results from these studies indicate that the changes occur during drying process in granulation step in a fluid bed of risedronate sodium. Moreover, they present feasibility of Raman for monitoring risedronate sodium (RS) which appear solid-state transformation during drying process in fluid bed. In addition, Raman spectroscopy is used to study the physical stability of the risedronate sodium tablets which occur solid-state changes during drying process in fluid bed (36).



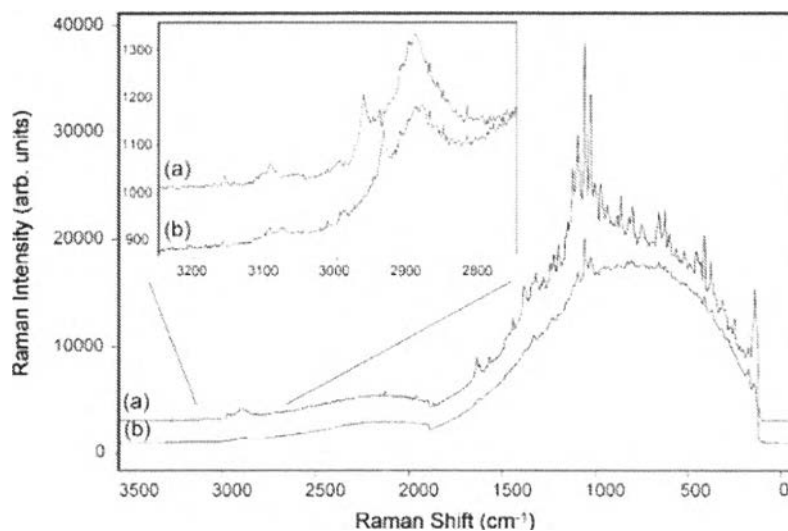


Figure 26 On-line Raman spectrum of drying process in granulation step at the start (a) and of drying process in granulation step until 1% moisture at the end (b) (36)

The best advantage of Raman spectroscopy that more than others spectroscopy is very poor interference of Raman scattering from water molecules. From this reason, this device is suitable to investigate any drug substances which have the water composition in the sample such as reactions in aqueous solution, biopolymeric and biomolecules material, little sample prepared by freeze drying, sample stored in desiccator or monitoring of living biological systems. On the contrary, IR spectroscopy obtains high interference with spectrum interpretation of IR absorption from water molecules due to occur vibrational of water band. Karmwar et al. exhibit the Raman spectra of all freshly amorphous indomethacin prepared by melt and quench-cooling method at various cooling rates shown in Figure 27. These results show broader peaks and merged of nearly peaks of all freshly prepared amorphous sample except Raman spectrum of the crystalline γ -form which shows sharply peaks because there are inherent variations in intermolecular bonding and molecular conformation within the amorphous structure. There are many different



peaks position are found between the crystalline structure and the amorphous forms which are previously observed by researchers but no observe spectra features of the amorphous samples similar to peak of the α - or γ -forms of the crystalline structure (2).

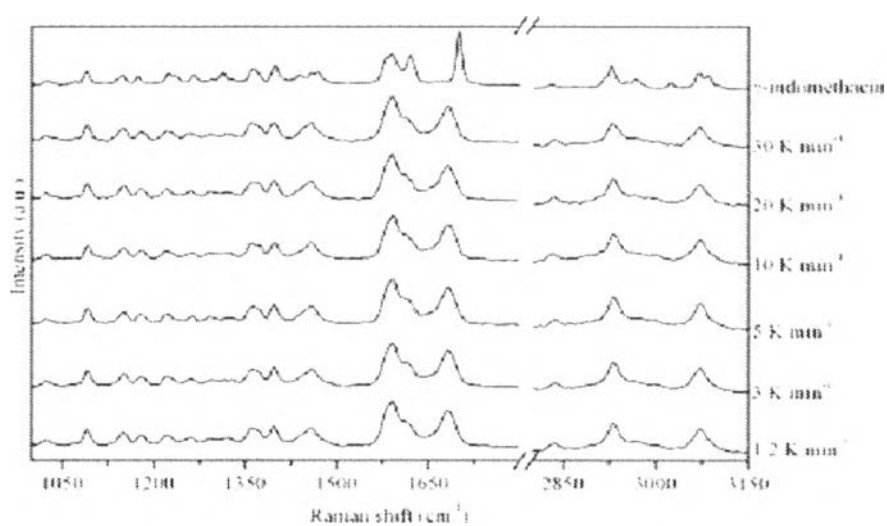


Figure 27 Raman spectra of amorphous indomethacin prepared by melt and quench-cooling method at various cooling rates (2)

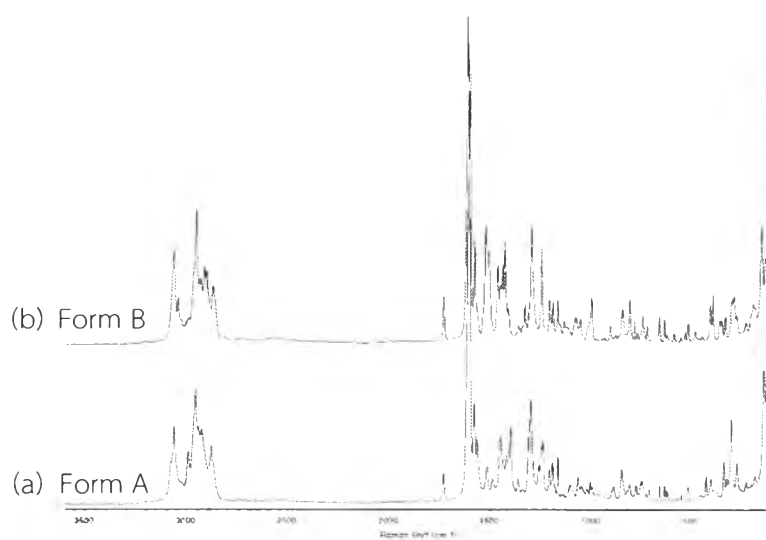


Figure 28 Raman spectra of developmental compound Form A (a) and Form B (b) (35)

Findlay et al. studied the differentiation between Raman spectra of developmental compound Forms A and B shown in Figure 28. These spectra exhibit that there are two various crystalline forms of developmental compound which can be differentiated by Raman technique. Moreover, this study can developed a new quantitative method using Raman technique for evaluating form B material mixing in bulk A material (35).

THEORY OF RAMAN SPECTROSCOPY

In 1930, the Indian physicist named Chandrasekhara Venkata Raman (C.V. Raman) discovered some of the visible wavelength of a small fraction that is scattered from the molecules changes in the wavelength compare to the wavelength traversed a transparent material. In addition, he discovered the shifts in wavelength that depend on the molecular bonding within structure responsible for the scattering radiation. This phenomenon is called Raman scattering and result from this phenomenon is called Raman effect (37).

Raman spectra are generated by sample irradiated from laser source of monochromatic radiation which usually uses in the visible or near-IR part of the electromagnetic radiation. The range of electromagnetic radiation is selected from high vibrational frequency but low electronic frequency. Usually, the scattering beam between the incident photon and the sample can be called elastic scattering which the vibrational and rotational energy of the molecule is unchanged. On the contrary, the Raman effect which is a type of beam scattering radiation can be considered as an inelastic scattering between the incident photon and the molecule. The vibrational or rotational energy of the molecule is changed in the inelastic scattering



(38). Figure 29 exhibits the differentiation of the Raman scattering observed in Raman spectroscopy compare to the light absorption observed from IR spectroscopy. In the Raman spectroscopy excitation wavelength involves with an absorption band and a virtual stage of energy level. A molecule in the ground vibrational level ($v = 0$) absorb a photon of energy ($h\nu_{ex}$) and reemit a photon of energy to the ground stage. In case of the scattered radiation is lower frequency than the excitation radiation, it is called Stokes scattering. On the other hand, the scattered radiation is higher frequency than the excitation radiation, it is called anti-Stokes scattering. Both of the Stokes scattering and the anti-Stokes scattering are inelastically scattering radiation caused a Raman signal. The elastic scattering radiation energy obtained from the emission of a photon equal to the energy obtained from the excitation of a photon. This scattering radiation of the same frequency is termed Reyleigh scattering shown in Figure 30 (37).

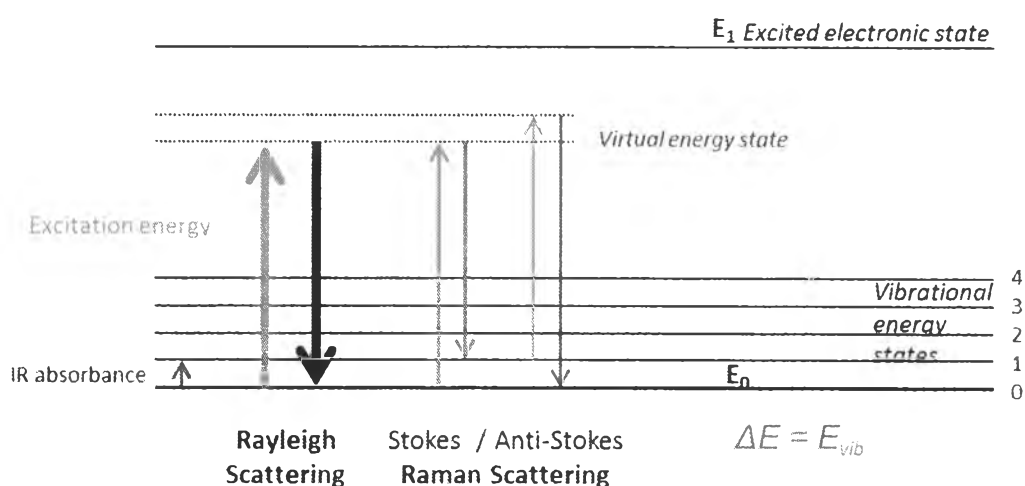


Figure 29 Schematic represents energy transitions in infrared and Raman spectroscopy (39)

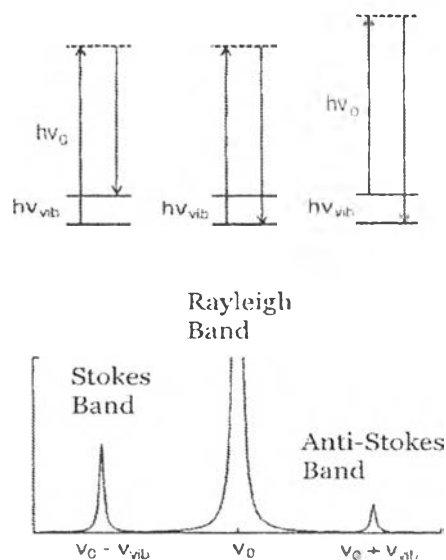


Figure 30 Schematic represents Rayleigh band, Stokes band and Anti-Stokes band of Raman scattering (40)

Figure 30 exhibits two bands found on both sides of the Rayleigh peak and one band on the center called Stokes bands, anti-Stokes bands and Rayleigh band, respectively (From left to right). Only the Stokes scattering of a spectrum is selected for evaluation due to Stokes lines has more intensity than Anti-Stokes lines and the magnitude is independent on the excitation wavelength. Usually, the Raman scattering radiation from the sample is evaluated at some angle (often 90 degree) with a suitable spectrometer. The intensities of Raman lines are obtained from 0.001% of the intensity of the excitation source. For this reason, it might seem more difficult to detect and measure Raman spectra than IR spectra but the Raman scattered radiation is in the visible or near-infrared regions which a lot of sensitive detectors are available. Therefore, the measurement of Raman spectra is nearly as easy as measurement of IR spectra.

INSTRUMENTS OF THE RAMAN SPECTROSCOPY

Raman spectroscopy involves irradiation with a laser at sample for collecting the scattered radiation and rejecting the Rayleigh scattered radiation. The Raman spectroscopy device consists of an excitation source, sample container device, a sample illumination system and a suitable spectrometer. The excitation sources utilized in Raman spectrometry are closely lasers due to this device is necessary to create Raman scattering radiation by high intensity from laser which have to sufficient intensity to be evaluated with spectroscopy. There are fifth of the most common lasers employed for Raman spectroscopy listed in Table 1 (37) and 2 (41).

Table 1 Laser type sources are used in Raman instrument (37)

Laser Type Source	Wavelength, nm
Argon ion	488.0 or 514.5
Krypton ion	530.0 or 647.1
Helium/Neon	632.8
Diode Laser	785 or 830
Nd-YAG	1064

Table 2 Lasers used in Pharmaceutical applications (41)

Laser λ , nm (nearest whole number)	Type	Typical Power at Laser	Wavelength Range, nm (Stokes Region: 100 cm^{-1} to 3000 cm^{-1} shift)	Comments
NIR Lasers				
1064	Solid state (Nd:YAG)	Up to 3 W	1075–1563	Commonly used in Fourier transform instruments
830	Diode	Up to 300 mW	827–980	Typically limited to 2000 cm^{-1} ; Raman shift because of CCD spectral response; less common than the other lasers
785	Diode	Up to 500 mW	791–1027	Most widely used dispersive Raman laser
Visible Lasers				
632.8	He-Ne	Up to 500 mW	637–781	Relatively small fluorescence risk
532	Doubled (Nd:YAG)	Up to 1 W	535–632.8	High fluorescence risk
514.5	Ar+	Up to 1 W	517–608	High fluorescence risk
488–632.8	Ar+	Up to 1 W	490–572	High fluorescence risk



There are two major processes are employed to collect the Raman spectra:

1. Dispersive Raman
2. Fourier Transform Raman (FT-Raman)

The both of processes have distinct in a type of laser and the detection and the evaluation processes of Raman scattering. Each processes has be specific advantages and disadvantages to analyzed sample shown in Figure 31 (42).

Dispersive Raman	FT-Raman
VIS : 785 nm, 633 nm, 532 nm, ... Grating Silicon CCD detector <ul style="list-style-type: none"> - higher sensitivity - higher spatial resolution for microscopy applications - lower laser power <ul style="list-style-type: none"> - minor component analysis - more sensitive for aqueous samples - analysis of dark samples - depth or cross-sectional information in samples 	Laser NIR : 1064 nm Spectral analysis by Interferometer Detector <ul style="list-style-type: none"> - room temperature indium gallium arsenide - liquid nitrogen-cooled germanium Advantages <ul style="list-style-type: none"> - limited fluorescence - maximal compatibility with libraries and analysis software Applications <ul style="list-style-type: none"> - in the pharmaceutical industry: <ul style="list-style-type: none"> - unknown identification - incoming raw material characterisation - final product quality - quantitative analyses - investigating polymorphs - forensic analysis through sample containers or evidence bags

Figure 31 Compared of dispersive and FT-Raman spectroscopy (42)

The basic instrumentations of a dispersive Raman spectrometer consist of laser, sample, grating and CCD shown in Figure 32. For dispersive Raman system, the visible wavelength lasers source is usually employed for Raman. The sample position of dispersive Raman instrument is selected in the focus of laser beam. The scattering radiations are created and collected in the direction at the 180 degree called the backscattering method or at the 90 degree called the right-angle method. Then, Raman scattering light radiated from sample pass into a diffraction grating. The diffraction grating will split the beam into its constituent wavelengths, whereas

Rayleigh scattering beam will be rejected by a laser-line rejection filter. Finally, the Raman scattering beam is measured by a suitable detector embedded in the spectrometer which is usually used as a silicon charge-coupled device (CCD) for the dispersive Raman systems.

Table 1 and Table 2 exhibit the fifth power of the frequency lasers source of monochromatic radiation which is usually employed in Raman spectrometer. There are fourth sources of laser in the table which emit visible radiation (argon ion, krypton ion, doubled continuous wave Nd-YAG and helium-neon) and give short excitation laser wavelengths that contain a much stronger Raman signal. Argon ion has wavelength at 488.0 or 514.5 nm, krypton ion has wavelength at 530.0 or 647.1 nm, doubled continuous wave neodymium yttrium aluminum garnet (Nd-YAG) has wavelength at 532 nm and helium-neon (He-Ne) has wavelength at 632.8 nm. Argon ion and krypton ion sources of laser give the blue and green region of the visible spectrum which has an advantage more than the other sources due to the argon ion source providing Raman intensity is three times the intensity observed from the He-Ne source at the same input power.

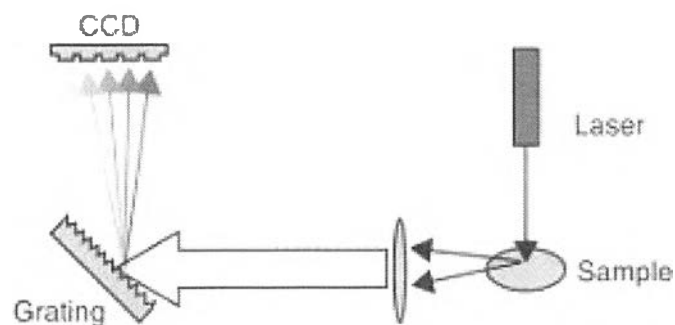


Figure 32 Schematic represents dispersive Raman spectroscopy (43)

Moreover, these short wavelength sources can produce significant fluorescence causing photodecomposition of the sample. In addition, there are two sources of laser in the table consisted of stabilized diode laser which has wavelength at 785 or 830 nm and the solid-state Nd-YAG which has wavelength at 1064 nm emit near-infrared (NIR) radiation. These two laser sources are always used in excitation sources of the modern Raman spectrometer. NIR laser sources have two advantages over visible laser sources. The first, NIR laser sources can be operated at higher power than visible laser sources without causing photodecomposition of the sample. The second, NIR laser sources are not energetic enough to create fluorescence scattering radiation which excited electronic energy states in molecules due to they use low energy compared to visible laser sources. The fluorescence effect depends on excitation wavelength therefore each samples occur fluorescence scattering radiation at the one wavelength and will not occur this situation at another wavelength. For these reasons, the Nd-YAG laser is effectively utilized in Fourier transform Raman (FT-Raman) spectrometers for eliminate problem from fluorescence scattering radiation. Moreover, diode laser source at wavelength 830 nm can clearly exhibits the reduction of fluorescence scattering radiation same results obtained from Nd-YAG laser source. Normally, the good spectrometers depend on the stability of the laser source which is a key property for evaluate samples and the good functional of tools. In addition, the cost and the lifetime of laser sources also consideration of choice to select the laser source. The high frequency laser can be selected to analyze for enhanced sensitivity in case of sample which want to enhance sensitivity and do not occur fluorescence scattering radiation. On the contrary, the low frequency laser (low energy source such as FT-Raman



spectroscopy) can be selected to utilize for reduce the fluorescence effects in case of sample which fluorescence scattering radiation is a problem when using high energy sources.

Some scientists suggest that all Raman spectra should be evaluated using the highest frequency or the shortest wavelength lasers which these conditions will be occurred a highly fluorescence scattering radiation due to fluorescence effect can be eliminated using software and other strategies to reduce fluorescence interference and still obtain the usable correct Raman spectra. However, Raman spectra cannot be measured in case of the fluorescence scattering radiation saturates the CCD (CCD overflow). The spectrum resolution is mean the amount of detail that can be observed in the spectrum. Therefore, it cannot impossible to distinguish between closely peaks if the resolution value is very low. The spectrum resolution is explained by the diffraction grating dispersion and by the optical design of the spectrograph. A lot of grating lines or grating grooves are blazed into the surface for help to disperse the incoming light. There are many processes to increase the spectrum resolution such as the higher number of grating lines per unit length or there are the broader the dispersion angle. In addition, all generated Raman scattering created cannot fall on the detector in one exposure if the detector size is fixed. Therefore, the method used to increase high resolution is either extend the optical path length of the spectrograph move the grating or improve the spectrograph design for collect all segments of the spectral.



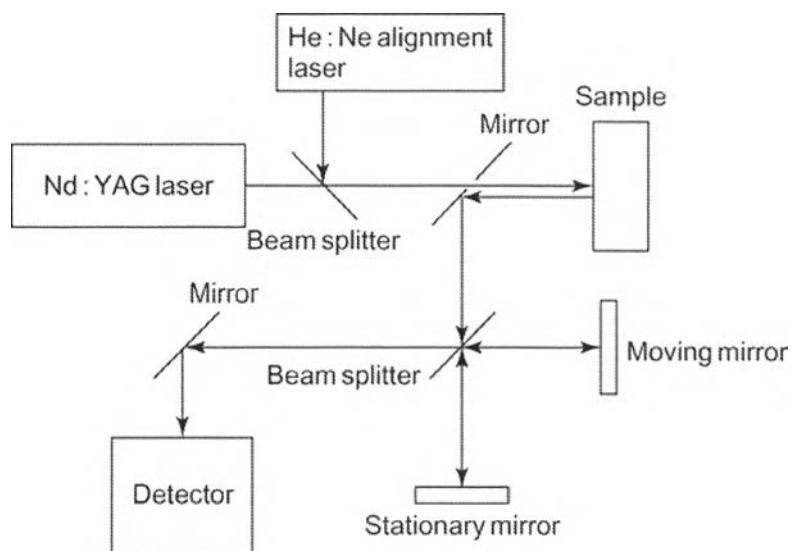


Figure 33 Schematic represents FT-Raman spectroscopy (44)

Figure 33 exhibits the basic configurations and components of the Fourier transform Raman (FT-Raman) spectrometer. The solid-state Nd-YAG laser which emits wavelength at 1064 nm is used to the energy source. This laser source virtually get rid of fluorescence and photodecomposition of samples according to above reasons. This advantage can be used to investigate dyes and other fluorescing compounds by FT-Raman instruments. Spectrum line is filtered by grating slit and focused on the sample. This result produces inelastically Raman scattering radiation from the sample and filter to eliminate the Rayleigh scattering. The laser beam is focused on sample cause the scattering radiations. These scattering radiations are collected in direction at 180 degree called the backscattering method or at 90 degree called the right-angle method similar to the dispersive Raman spectroscopy. The scattering radiations are moved into an interferometer pass laser line filtering. The optical filtering is a necessary part in the interferometer. The interferometer of the FT-Raman has many advantages compare to grating of dispersive Raman. The



grating is monochromator of equal aperture where radiation pass through narrow slits compared with the larger optical conductance of an interferometer. The stray light from the exciting laser must be eliminated because it can saturate many transducers. The Rayleigh scattered line is often six times of magnitude higher than the Stokes shifted Raman scattering radiations and the intensity of this line must be minimized before striking the transducer by holographic notch filters and other filter types. Most FT-Raman instruments instead use indium doped with gallium arsenide (InGaAs), high purity *p*-type germanium (Ge) and other photoconductive devices as transducers. This device is usually operated at cryogenic temperatures by generally liquid nitrogen cooled. In the modern instrument, this device can be evaluated at room temperature due to there is develop a program to help compensate of the signal-to-noise ratio. InGaAs transducer is the most used to detector of the FT-Raman. This detector is more noise than the CCD detectors of the dispersive Raman but it exhibits quantum efficiencies more than CCD detectors.

The most advantages of the FT-Raman spectrometer produce accuracy and precision wavelength. In addition, a NIR laser is used to eliminate the false effects from fluorescence scattering. The FT-Raman instrument also provides higher frequency precision compare to dispersive Raman instrument. On the other hand, the disadvantage of the FT-Raman spectrometer is water absorbs in the 1000 nm region lead to this device does not be able to use with the samples that have aqueous compositions. Furthermore, the Raman scattering from Nd-YAG laser can occur at wavelengths as long as 1700 nm caused photomultipliers and many array detectors are not used.



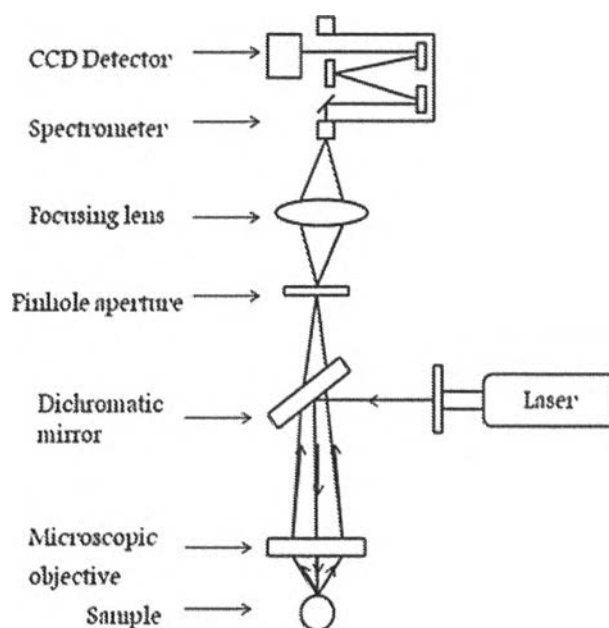


Figure 34 Schematic represents confocal Raman microscopy (45)

Another type of Raman spectroscopy is confocal Raman microscopy which brings Raman spectroscopy fuse with a microscope (confocal imaging) to provide capabilities. The chemical information about a small area of the sample can be obtained from this instrument. This is the best advantage over the conventional Raman spectroscopy. The Raman spectrum from confocal microscopy gives information through various techniques such as transmission, reflection, emission, absorption, photoluminescence or fluorescence. The confocal Raman microscopy bases on the inelastic scattering of monochromatic light when laser source focus on the sample and the energy of photons changes lead to interaction within molecule. The solid preparation of pharmaceutical dosage form such as tablet can be evaluated using a confocal Raman microscope to scan all of point cover the surface of the sample called Raman mapping. Figure 34 exhibits confocal Raman microscopy which is the best device with short wavelengths. This device is utilized to investigate



heterogeneous systems on the micrometer scale by non-destructive sample technique. Light from other depths in the sample (above or below the focal plane) is not collimated by the objective and will be defocused at the pinhole. Therefore, this technique is suitable to collect a data from a single point on a sample. The confocal Raman microscopy consists of laser, sample, microscopic objective, dichromatic mirror, pinhole aperture, focusing lens, spectrometer and CCD detector. In the beginning, the laser light source from the probe head focuses on diffraction limited spot on the sample through the microscopic objective. It can choose any position that give XYZ-location (three dimensional locations) on a sample with a resolution value in the micron range. The confocal points are only located of the point source, the focus sample place location and the image point of the sample. Moreover, a signal spectrum can be transformed information about the chemical composition of the given spot on a sample. Furthermore, there are two types of resolution which consist of depth resolution and axial resolution. The depth resolution is defined as the distance from the focal plane that there is maximum Raman intensity until the in-focus sample position that there is Raman intensity decrease to 50% off. This distance can be approximately measured from the numerical aperture used in the microscope. On the contrary, the axial resolution and optical slicing of a sample are determined by the reduction of the out of focus signal or by size of a pinhole that limits the signals come out from exterior focus zones. The choice of a slit or pinhole entrance of the detector stage depends on the resolution and signal intensity desired. If a pinhole is chosen to obtain optimal resolution, the signal intensity may be too low. Therefore, a larger pinhole and consequently laser resolution may then be selected (46). The Raman scattering light from the sample is collected with the



same objective which compensated the excitation radiation. The backscattering of Raman signal is refocused on a pinhole aperture which function is a spatial filter and passes the excited Raman signal at the beam waist in direction at the 180 degree. In addition, this process can be eliminated Raman signal produced from other points above and below the beam waist. All above reasons, the backscattering Raman signal is employed in confocal Raman microscopy for evaluate the Raman spectrum from the sample surface without sample preparation. The filtered Raman signal and remained Raman scattering come back to the spectrometer and then it is scattered on a CCD camera to create a Raman spectrum (45).

The disadvantage of confocal Raman microscopy is a very weak incident peak of Raman scattering. Therefore, this equipment is necessary to improve for well-established method of chemical analysis in the field of molecular spectroscopy. In contrast, the outstanding advantage of confocal Raman microscopy is not need sample preparation and help to improve axial and depth resolution compare to conventional Raman spectroscopy lead to exhibit extremely detailed analysis of sample. Moreover, the macroscopic resolution possible to investigate the chemistry mapping of individual sample for generated images. The pharmaceutical industry use confocal Raman microscopy for characterize the structure and show the detail of the active components on the surface, exhibit chemical mapping of pills and tablets and investigate homogeneity tests of creams and ointments (47).

CHEMOMETRY

Chemometrics is the application of mathematical or statistical science method in order to extracting information from calculation on measurements of



chemical data using data-driven means. There are many techniques for collecting good data and for getting information from these data. These data obtained from hundreds to thousands of experiments are more than hundreds to thousands of variables. Some final datasets have a small quantity but there are very large and highly complex on this test. Chemometrics tries to build a bridge between the methods and their variables. This method is frequently employed in data analysis principle such as multivariate statistics, computer science and applied mathematics so as to solve the problems in chemistry, biochemistry, medicine, biology, chemical engineering and prediction the final result from experimental testing.

Chemometrics knowledge can be employed to solve both descriptive and predictive issues of life sciences especially in experimental design of chemistry. In descriptive applications, the chemometrics are used to investigate systems that are modelled to learn the underlying relationships and system structure. In predictive applications, the chemometrics are used to predict the new target properties, desired features or behavior of interested sample.

MULTIVARIATE ANALYSIS

A multivariate measurement is multiple measurements evaluated on a group sample of interest. Multivariate variation is based on the statistical discipline of multivariate statistics that entails with observation and data analysis of different statistical variable outcome at a time. Each sample involves more than a single variable or response measured by each situation. This technique is used to execute studies across multiple dimensions whereas taking the effects into all variables on the interesting responses.



Multivariate data analysis is the process that involve with extracting information from a data matrix. There are many purposes that evaluate with various multivariate data analysis techniques. One of the purposes is prediction in behavior of interest called data exploration, supervised or unsupervised pattern recognition. The data exploration is used to predict data for survey interesting situation by without previous expectations. Outliers from this method may be detected and be deleted out of overall sample for correct calculation.

Moreover, the pattern recognition is a one of the most success in multivariate data analysis. A lot of knowledge of sciences especially department of chemistry involves with large amounts of data which can be determined by pattern classification or pattern recognition. Pattern recognition consists of unsupervised pattern recognition and supervised pattern recognition. There are many methods such as Raman spectroscopy, IR spectroscopy, NIR spectroscopy or chromatography (HPLC) that require chemical pattern recognition to classify group of data.

UNSUPERVISED PATTERN RECOGNITION

Unsupervised pattern recognition is usually the formal method for treating samples which are usually called cluster analysis. The cluster analysis evaluates patterns of data which relate to data attributes with a class attribute. This pattern is tool to predict the interesting values of the target attribute in future data instances. A lot of methods have the origin in numerical taxonomy by biologists. Some parameter is used to separate a lot of sample such as body length. The various species which are most similar will be drawn as a group of picture of these similarities called a dendrogram shown in Figure 35 (48). This dendrogram shows that nearly related



species are closer to each species. For example, group no. 2 sample is similar to group no. 5 sample more than group no. 4 sample.

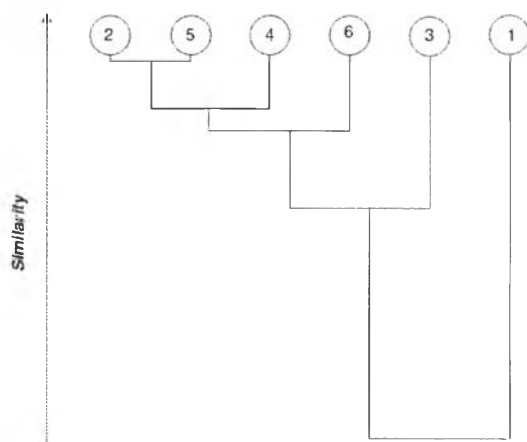


Figure 35 Schematic represents dendrogram (49)

The unsupervised pattern recognition principles can be used to chemical sciences. For example, it can be possible to explain similarities and dissimilarities in amino acid sequences within myoglobin of the various species from The Tibetan antelope (TA) and other species shown in Figure 36. The result indicates that the TA myoglobin is more related to *Ovis aries* than *Bos Taurus*. The similar species have the closely in relationship both chemical and biological similarity (50). The cluster analysis of unsupervised pattern recognition is only practicable way to separate the amount of information from a large genomic or from crystallographic databases. Then, data obtained from cluster analysis is classified by other mathematical statistic for predict behavior of interested sample.



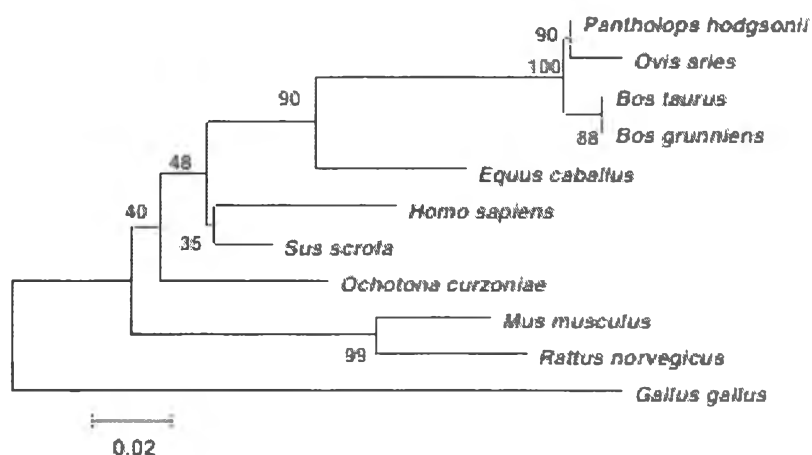


Figure 36 Dendrogram of amino acid sequences within myoglobin of the various species from the Tibetan antelope (TA) and other species (50)

SUPERVISED PATTERN RECOGNITION

The supervised pattern recognition is utilized to evaluate for many reasons. One of the most aims is classify unknown data. Only one measurement or single run give information not enough therefore a lot of parameters are required for create mathematical model. The statisticians develop a large number of discriminant functions. Each data does not target distribution lead to discover the data to predict some intrinsic structures within them. In case of spectroscopy technique is chemical method used to decide the suspense data. In the beginning, the method can be clearly classified spectra to two groups. All spectra data are set up by mathematical statistic called mathematical model or training set. Then the unknown sample can be predicted using created mathematical model.

The supervised pattern recognition is technique that create a training set for predict to the class of an unknown sample. The training set is a set of known groupings data that available in advance. There are many benefits of the supervised



pattern recognition. This technique is utilized to chemical measurements which are actually good enough to match into the predetermined groups. Moreover, spectroscopic or chromatographic processes for diagnosis are usually more valuable and cheaper than medical testing process due to the chemical pattern recognition helps quickly screening sample without doubt. Furthermore, this technique is applied to the pharmaceutical industrial process control for help improve and increase products due to the control and routine batches might be investigated at all the time or divide interval. Therefore, on-line testing sample using any method is important first step to collect chemical data and to determine the possible acceptability of a batch.

EXPLORATORY DATA ANALYSIS

The exploratory data analysis (EDA) is a tool for analyze data sets in order to extract their major and minor characteristics of sample especially using visual methods. This technique is similar to unsupervised pattern recognition. The differentiation between the exploratory data analysis (EDA) and the unsupervised pattern recognition is the aim of these methods. The unsupervised pattern recognition is used to detect similarities. On the contrary, the EDA is used to classify that how many groups will be found by without bias. The EDA is mainly composes of the two techniques namely Principal Components Analysis (PCA) and Factor Analysis (FA).

PRINCIPAL COMPONENTS ANALYSIS (PCA)

The Principal Components Analysis (PCA) is the most famous multivariate statistical technique used in chemometrics. The PCA is a mathematical manipulation



of a data matrix or a statistical procedure concerned with elucidating the covariance structure of a set of variables (dimensionality reduction). A small number of factors is the final result that represents variation in various variables. The original data or measurement variables are redefined by the axes using suitable factors lead to a new row space is constructed. Each new constructed axes is called factors or principal components (PCs). The first principal component (PC1) accounts for maximum proportion of variance from the original dataset.

PCA can be best understood using a simple two variable example. If there are only two variables, it is possible to plot the row space without the need to reduce the number of variables. Although this does not fully present the utility of PCA, it is a good demonstration of its functions. Figure 37 shows the data matrix that consists of 2 columns representing the two measurements and 16 rows representing the samples. This figure indicates the first principal component (PC1) is slightly more parallel to the variable 2 axis than to the variable 1 (51).

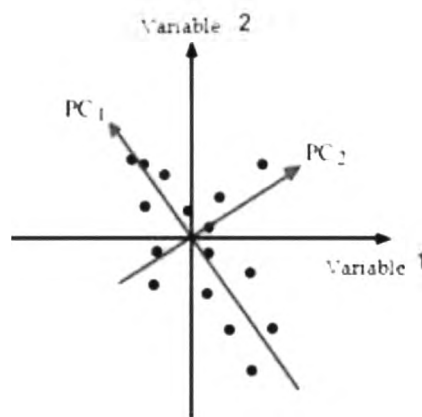


Figure 37 A row plot of data in a two-measurement system (Variable 1 and 2) with the first two principal component axes (PC1 and PC2) (51)

It is interesting study the relationship between the samples in the row space and the distances between samples are used to define similarities and dissimilarities. The goal of PCA in mathematical terms is described as the interpoint distances either spread or variation using a possible few axes or dimensions. This is accomplished by constructing PC axes that align with the data. The first principal component (PC1) explains the maximum amount of variation found in the data set in one direction, in other words, it is the direction which explains the maximum spread of data points or the direction in space along which projections have the largest variance. In addition, the second principal component (PC2) is the direction which orthogonal to the first PC (PC1). Furthermore, the percent of any principal component (PC) can be precisely calculated from sum of each variation in the dimension of the data set.

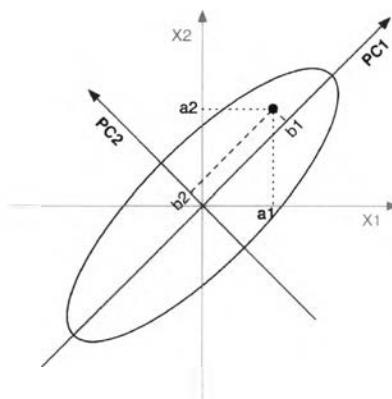


Figure 38 The coordinates of one point relative to the original axes (the dotted lines) and the principal component axes (the dashed lines) (52)

If closely to 100% of the variation is described using two PCs, a two-dimensional plot can effectively be used to study the variation in the data set. On the contrary, a two-dimensional plot will not be adequate if only 20% of the variation is described indicating that too much variation is missing.



The sample has coordinates in the original row space which is defined by the original variables data therefore it also has coordinates with respect to the new PC axes. These can be found by drawing a perpendicular line from the sample to the principal component axes shown in Figure 38. The dot line shows the coordinates of one sample correspond to the two original variable axes (a_1 and a_2) and the dash line shows the coordinates of that sample associated with the first principal component (PC) axes (b_1 and b_2). The coordinates of the samples correspond to the principal component axes are called in mathematical termed as scores.

Each original measurement variable is calculated and separated as each PC. Each original measurement variable is contributed to each PC depends on the associate with orientation in space of each PC and variable axes. Therefore, each PC is constructed from diverse variables. Figure 38 indicates that one variable (black spot) is slightly more parallel to the PC1 axis than to the PC2 axis. For above interpretation, it is useful to know that each variable is contributed most significantly to the individual principal components, in other words, there are the constructed axes that are potentially the best fit at discriminating between samples.

In mathematical terms, the contribution of each axis to a principal component is the cosine of the angle called $\cos \theta$ between the variable axis and the principal component axis. If principal component points exactly in the same direction as an individual variable, the angle between them is 0 caused the cosine is 1 indicating that the PC describes all of the variation in that variable axis. Similarly, if a principal component is perpendicular to an individual variable axis, the angle between them is 90 caused the cosine is 0 indicating that none of the variation is



contained in the PC. All above reasons indicate that these cosine values can range from -1 to 1 called in mathematical terms as loadings.

The principal component analysis (PCA) is an excellent technique that transforms the large data space of all dataset in the ixj matrix into a smaller space which is easier to interpretation shown in Equation 2.

$$X = t_1p_1' + t_2p_2' + \dots + t_Ap_A' + E \quad (\text{PCA Equation 1}) \quad (\text{Equation 2})$$

Where X is an (ixj) matrix which is usually passed treatment by data preprocessing. The t_A is a scores values for the A^{th} component, the p_A is a loading values for the A^{th} component and E is the (ixj) residual matrix. A is a latent variable which is general name for the principal components (PCs). The sum of squares of X with a possible lower number of PCs is the final target of PCA. This equation is completed when both t_A and p_A represent the orthogonal and the orthonormal, respectively. There are two important things that to know about final target of PCA technique. First, the suitable number of the sum of squares of X goes into the model. Another, how much is left in the residual. The noise must be clearly separated out of the residual especially in case of the noise is largely left in the residual.

The PCA is a convenient technique because this technique is accurate, fast and gives a unique result. On the other hand, there is one of the most important problems by PCA technique is the suitable of the number of principal components (PCs) to be used (amount of A). Generally, the two dimensional plot can effectively be used to study the variation in the data set when summary of selected two PCs closely to 100% of the variation (53).



CHEMICAL FACTORS

Equation 3 exhibits PCA equation in mathematical terms which is transformation data from the original data matrix to PCs axis as follows

$$X = T.P + E \quad (\text{PCA Equation 2}) \quad (\text{Equation 3})$$

Where: T is the scores matrix containing rows number equals to the original data matrix

P is the loadings matrix containing columns number equals to the original data matrix

Limitation: The columns number of the matrix T must be equals to the rows number of the matrix P

It can be calculated the scores and the loadings matrices as large as desired but the usual dimension is not larger than the dimension of the original data matrix. This is a limitation of dimension matrix. For example, there is the original data matrix is dimensions 5×7 (ixj), therefore the number of calculated PCs are not more than 7. The number of PCs in this case is assumed by A, therefore this number cannot more than 7.

The T matrix consists of the dimensions $5 \times A$ (ixj)

The P matrix consists of the dimensions $A \times 7$ (ixj)

Figure 39 shows data transformation as two group vectors (scores matrix and loadings matrix) by PCA technique. Each scores matrix composes of a series of column vectors ($1 \times A$) while each loadings matrix consists of a series of row vectors



($A \times J$). The scores matrices T ($I \times A$) and the loadings matrices P ($A \times J$) are comprised of several vectors. Each constructed vector is equal to each principal component (A). Many mathematicians indicate these vectors by t_A and p_A , where A is the number of the principal components (1, 2, 3 up to A). Each serial component is obtained from matching of eigenvectors. Therefore, the first scores vector and the first loadings vector are usually called the eigenvectors of the first principal component (PC1).

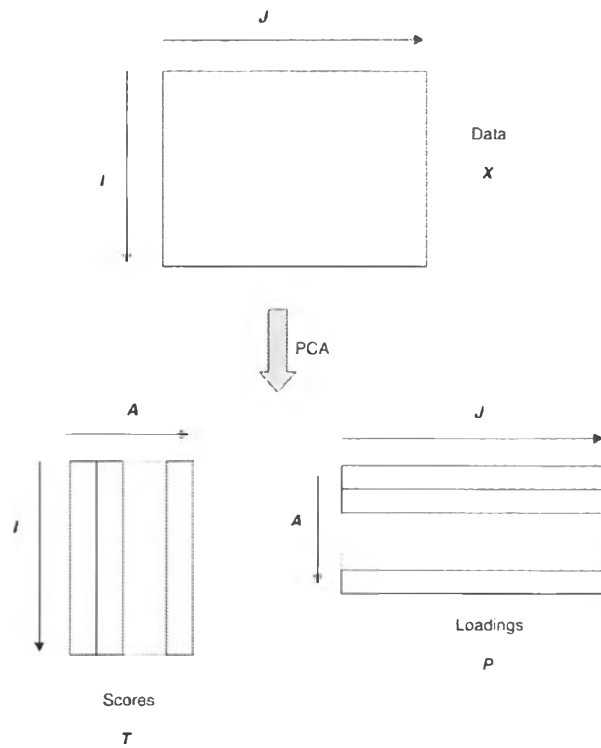


Figure 39 Schematic represents data transformation by PCA technique (49)

Figure 40 shows the data simplification transformation by PCA technique. The original variables are transformed to a number of significant principal components (PCs). This technique can be utilized as the format of variable reduction. The reduction method is a process used to reduce the large original dataset to a small dataset which is more manageable and more easily to interpretation. The best

important and aim of PCA technique involves with the searching mathematical correlations which contain some properties correspond to chemical factors within sample and agree with themselves.

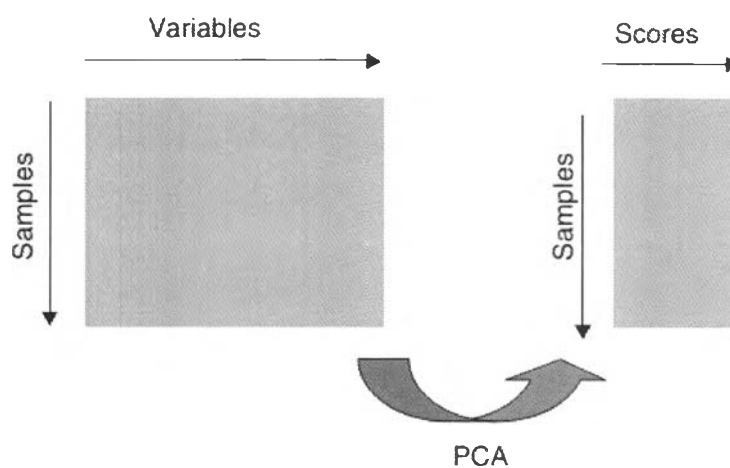


Figure 40 Overview of data transformation by PCA technique (49)

DATA PREPROCESSING

Before evaluation by mathematical statistic, all chemometrics data are treated by the suitable method for preparing information called the data preprocessing. This method is the first steps in data preparation. The process is necessary for correct or improve the original data to accuracy for interpretation by multivariate data analysis. The data preprocessing is a very important section for any chemometrics data analysis technique because it is a first process used to any mathematical manipulation of the data before these data will be brought testing by PCA technique. It is a method to remove or reduce unrelated sources of variation by either random or systematic. The data preprocessing transforms the data which will either positively or negatively influence to the results.

Selecting the optimal data preprocessing may require some iteration between the primary analysis and the preprocessing step. Although this empirical approach is a common practice, it is best if the preprocessing tool is chosen because of a known characteristic of the data.

Data preprocessing tool is separated into two basic types which depend on it operate on samples or variables. Sample preprocessing tools operate on each one sample at a time over all variables. In contrast, variables preprocessing tools operate on one variable at a time over all samples. Therefore, if a sample is deleted from a data set, variable preprocessing calculations must be repeated, while the sample preprocessing calculations will not be affected.

There are four methods of data preprocessing tools. First, normalization method can be used to remove sample to sample absolute variability such as variable from injection volumes in chromatography. Second, weighting method emphasizes selected samples over others. Third, smoothing is primarily used to reduce random noise, whereas the other sample preprocessing methods are used to remove systematic variations. The last, baseline features method can be removed using explicit models, derivatives or multiplicative scatter correction.

GRAPHICAL REPRESENTATION OF SCORES AND LOADINGS

The modern innovations in chemistry correspond to the graphical presentation of information such as bar graph, scatter plot or 3D plot. The modern computer is easy to convert from number of the statistical data to graphs. A lot of modern multivariate statisticians have a concept idea about geometrical format equal to numerical format. The concepts such as PCA are usually considered as



objects in an imaginary space rather than mathematical entities. The multivariate analysis statistics are similar to the algebra of multidimensional space. It is suitable to obtain a graphs quickly using simple software especially Microsoft Excel program. There are many methods of visualizing PCs but only the created first two PCs (PC1 and PC2) for graph expression is simplicity (two dimensions). There are two types of graph expression by PCA technique are scores and loadings plot.

SCORES PLOTS

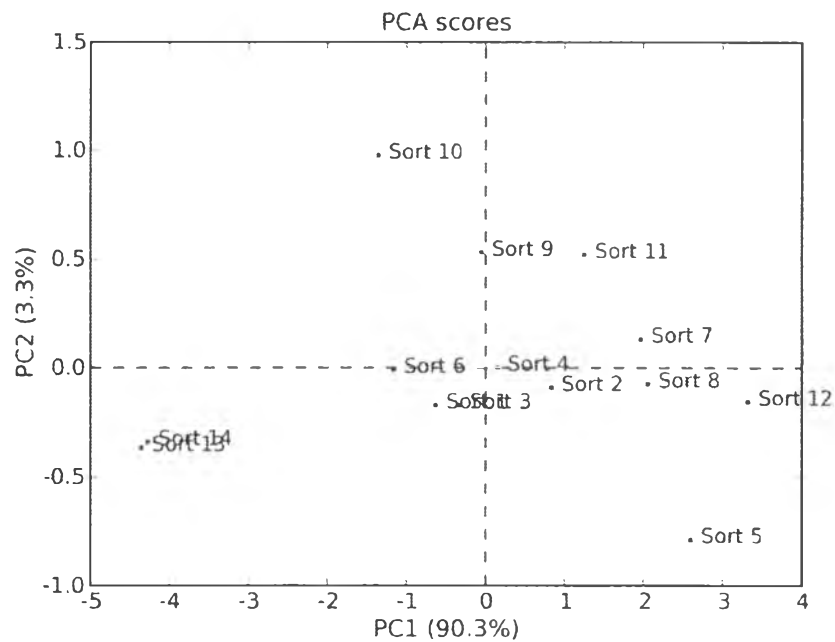


Figure 41 Scores plot of the first two PCs [PC1 (horizontal axis) versus PC2 (vertical axis)] (54)

The scores plot of PCA represents the score of the one PC against another PC. Figure 41 indicates scores plot of the PC1 versus the PC2. The horizontal axis exhibits the scores of the first PC (PC1) accounted for 90.3% of overall variance and the vertical axis indicates the scores of the second PC (PC2) accounted for 3.3% of

overall variance. The scores plot is a projection of data onto subspace. It is used for interpreting relations among observations.

Kao et al. observe the recrystallization of γ -indomethacin (IMC) from amorphous IMC. They evaluate a range of crystallization at various conditions using a combination of technique such as DSC, Raman spectroscopy, NIR spectroscopy and PCA. There are three samples prepared by different method consist of ball milled, melt and quench-cooled, and melt and quench-cooled with 5% (w/w) of crystalline seeds. Figure 42 shows Raman spectra of amorphous indomethacin, crystalline α - and γ -indomethacin. Figure 43 shows NIR spectra of amorphous indomethacin, crystalline α - and γ -indomethacin. The emphasized region in the NIR spectra is used for PCA as it provided the most significant results. The data are collected at above all the time points from the three samples and are storage under the three conditions (25°C dry, 40°C dry and 40°C 75%RH). All these data are transformed by mean-centered method of data preprocessing technique to both Raman and NIR spectra and then are analyzed in a single PCA shown in Figure 44. This figure exhibits the scores plot of PC1 (accounted for 77% variance) versus PC3 (accounted for 6% variance) of data from all NIR spectra corresponded to percentage amorphous content obtained from DSC technique. Figure 44 shows score plot calculated from NIR data. The distribution of amorphous content is not clear when compare to score plot obtained from Raman spectroscopic data. The recrystallization from amorphous sample to crystalline IMC is observed along PC3 rather than PC2 compare to PC1 (5).



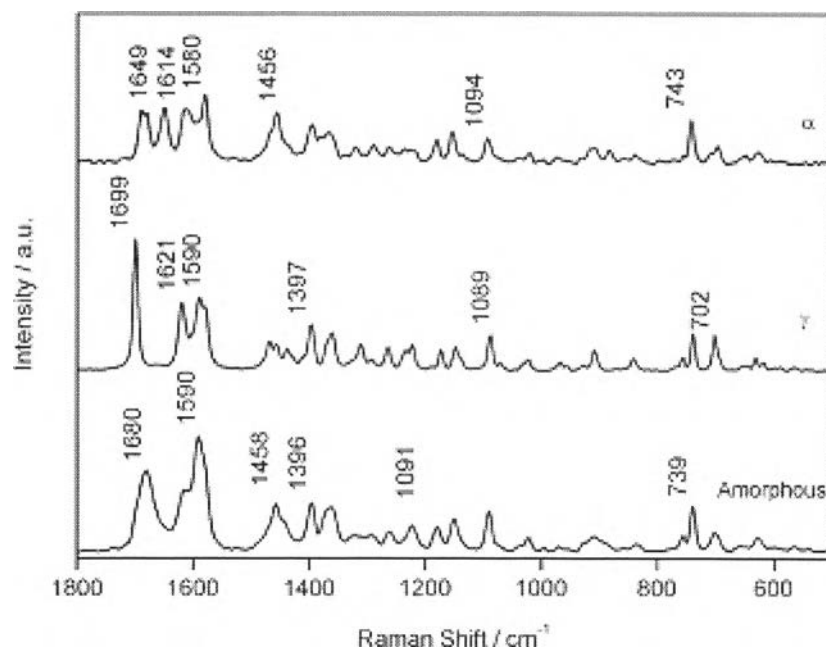


Figure 42 Raman spectra of amorphous, α - and γ -indomethacin (5)

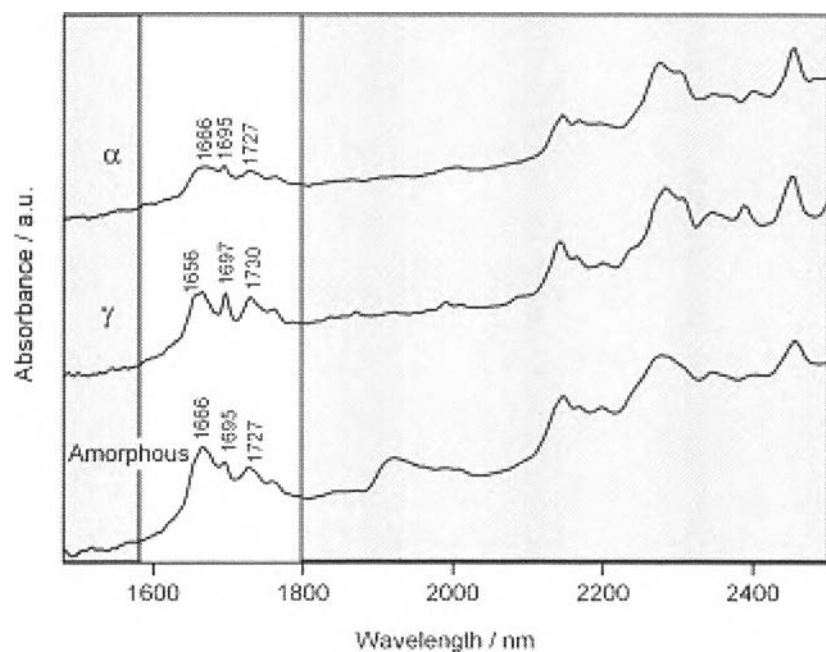


Figure 43 NIR spectra of amorphous, α - and γ -indomethacin (5)



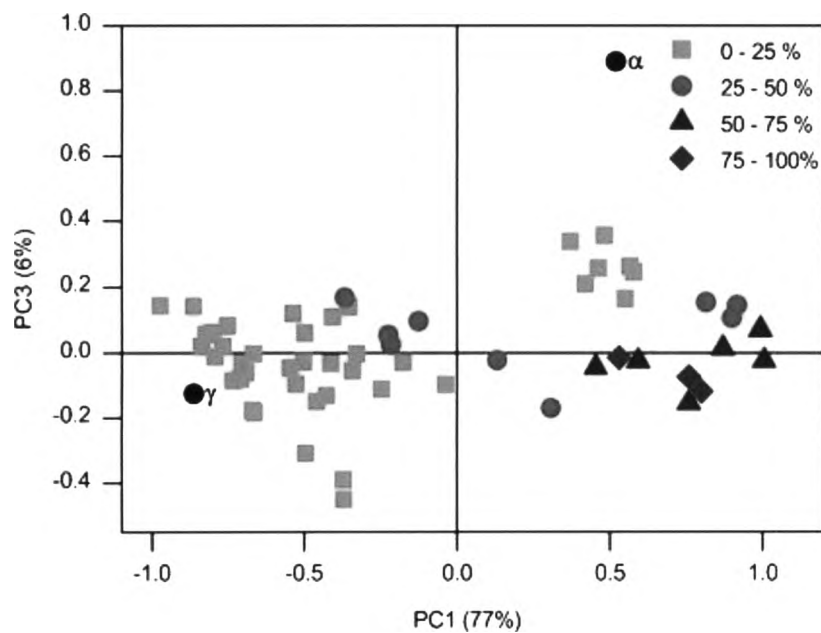


Figure 44 Scores plot of PC1 (accounted for 77% variance) versus PC3 (accounted for 6% variance) of data from all NIR spectra corresponded to percentage amorphous content obtained from DSC technique (5)

Dukeck et Al. investigate and correlate of physical stability, dissolution behavior and interaction parameter of amorphous solid dispersions of telmisartan. Figure 45 shows the scores plot (three dimensions) of the PXRD diffractogram of all freshly amorphous telmisartan prepared and stored by various proportion polymers. This diffractogram reveals the movement of the stored samples from the cluster of freshly prepared amorphous telmisartan to the crystalline or semi-crystalline solids (as a function of time and polymer used (55).



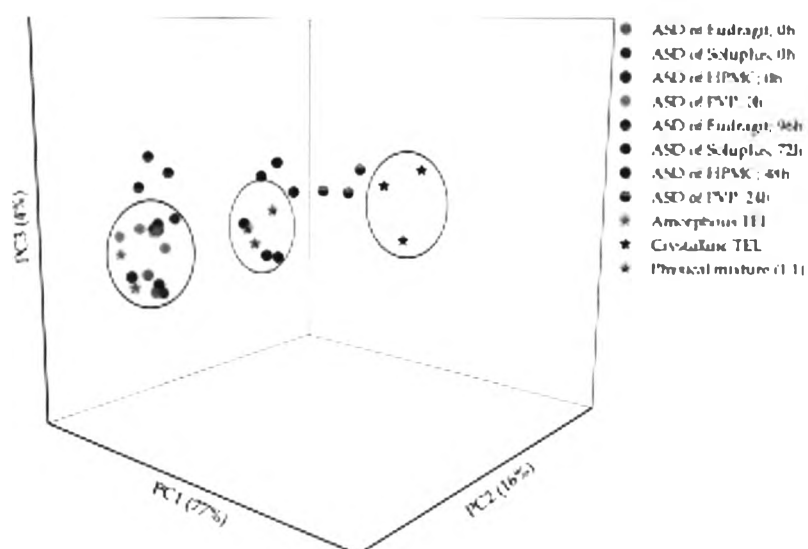


Figure 45 Scores plot of the PXRD diffractogram of all freshly amorphous telmisartan prepared and stored by various proportion polymers (55)

LOADINGS PLOTS

The loadings plot of PCA represents the loading of one PC against another PC. The loadings plot is a plot of the relationship between original variables and subspace dimensions. It is used for interpreting relationships among variables.

CLUSTER SEPARATION INDICES (CSIs)

The excessive number of samples usually resulted from various number of variables. It is not possible to rely only on the Mahalanobis distance measurement as to construct cluster separation indices (CSIs). Therefore, all the raw data are reconstructed as the simulated data sets which consist of only two variables by PCA. The scores of the first two PCs are result from each PCA. CSIs are used to check the results obtained by unsupervised cluster analysis such as PCA. The CSIs can be separated into two classes. One class uses low values for the determination of CSI

and another class uses high value for the determination of CSI for optimal separation (56).

THE DAVIES BOULDIN INDEX (DBI)

The Davies Bouldin Index (DBI) is usually employed for the determination of CSIs for a small sample number which indicates optimal separation. The DBI is based on a ratio of within cluster and between cluster distances of the sample. The DBI is defined as

$$DBI = \frac{1}{2} \left(\frac{d_2(A) + d_2(B)}{d(A, B)} \right)$$

Where $d_2(A)$ is the average Euclidean distance between each point of samples A and the centroid of the cluster A (intra-cluster distances A)

$d_2(B)$ is the average Euclidean distance between each point of samples B and the centroid of the cluster B (intra-cluster distances B)

$d(A, B)$ is the Euclidean distance between the two centroids of two clusters (inter-cluster distances between two clusters)

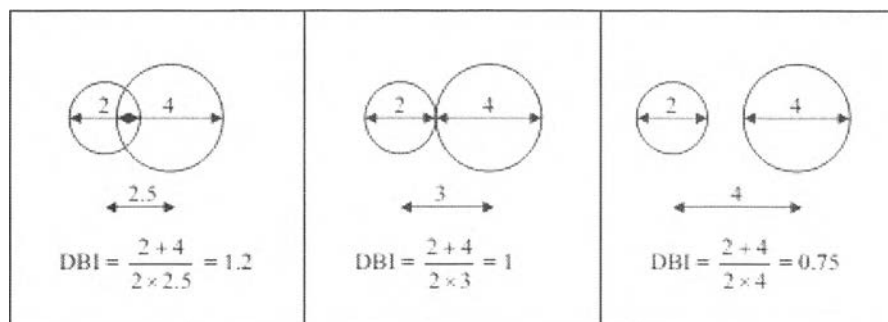


Figure 46 Example calculations of the DBI by assume perfectly spherical clusters

Figure 46 show example calculations of the DBI by assuming perfect spherical clusters. The limitation of DBI is the assumption of analysis of only perfect spherical

clusters. The average distance of each sample point compare to its centroid is calculated as the width of the cluster which is usually the widest point and is the limitation of this method. If the value of the DBI equal 1, it means that the edges of the two clusters are touching. Moreover, if the two clusters are overlapping, the divisor will be a lower value caused DBI to be high (DBI value > 1). If the two clusters are exactly overlapping or the level of overlap of the two clusters are close together (the sample mean between two clusters is nearly equal), the divisor will be nearly zero caused DBI to be maximum or theoretically reading infinity. Furthermore, if the two clusters are exactly separated, the divisor will be high caused and DBI will be minimum (DBI < 1) (56).

